

The Resistance Committee

Final Report and Recommendations to the 25th ITTC

1. INTRODUCTION

1.1 Membership

Chairman:

Dr. Emilio F. Campana
Istituto Nazionale per Studi ed Esperienze di
Architettura Navale (INSEAN), ITALY

Secretary:

Dr. Joseph Gorski
Naval Surface Warfare Center, Carderock
Division, UNITED STATES OF AMERICA

Members:

Dr. Ho-Hwan Chun
Pusan National University, KOREA

Dr. A. H. (Sandy) Day
Universities of Glasgow and Strathclyde,
Scotland, UNITED KINGDOM

Dr. De-Bo Huang
Harbin Engineering University, CHINA

Mr. Gregor Macfarlane
Australian Maritime College, AUSTRALIA

Dr. Tommi Mikkola
Helsinki University of Technology, FINLAND

Dr. Yusuke Tahara
Osaka Prefecture University, JAPAN

Dr. Jesús Valle
Canal de Experiencias Hidrodinámicas de El
Pardo (CEHIPAR), SPAIN

1.2 Meetings

The committee met 4 times:

6-7 February 2006, Launceston, Australia

16-17 September 2006, Rome, Italy

3-4 May 2007, Valencia, Spain

11-12 December 2007, Bethesda, United States

1.3 Tasks

Below we list the tasks carried out by the 25th resistance committee (RC), based on the recommendations given by the 24th ITTC.

1. Update the state-of-the-art for predicting the resistance of different ship concepts, hull design methods and hull optimization emphasising developments since the 2005 ITTC Conference.
 - a) Comment on the potential impact of new developments on the ITTC.
 - b) Emphasise new experimental techniques and extrapolation methods and the practical applications of computational methods to resistance prediction and scaling.
 - c) Identify the need for R&D for improving methods of model experiments, numerical modelling and full-scale measurements.
2. Review ITTC recommended procedures 7.5-01-01-01 and 7.5-02-02-01 to 7.5-02-02-06.
 - a) Determine if any changes are needed in the light of current practice.



- b) Identify the requirements for new procedures.
 - c) Support the Specialist Committee on Uncertainty Analysis in reviewing the procedures handling uncertainty analysis.
3. Critically review examples of validation of prediction techniques. Identify and specify requirements for new benchmark data.
 4. Complete the ITTC worldwide comparative tests for establishing benchmark data to identify the facilities biases.
 5. Identify developments in computational and experimental methods for prediction of far field waves and wash.
 6. Review experimental and computational methods to describe the airflow around the superstructure of vessels.

2. RESISTANCE COMMITTEE QUESTIONNAIRE

The RC was charged with updating the procedures for model manufacture (7.5-01-01-01) and for resistance tests (7.5-02-02-01). In some cases, improvements could be made in wording and notation; however some areas appear to offer the potential for technical improvements.

In order to inform others of the process of updating the procedures the RC prepared a questionnaire on issues considered by the RC to offer potential for improvement. This addressed three areas: Turbulence Stimulation, and Scaling; Speed Measurement, and Model Installation. The questionnaire was circulated by e-mail to all ITTC facilities. 25 facilities replied to the questionnaire; 11 from Europe, 11 from Asia and Australia and 3 from the Americas. Not all facilities answered all questions. The RC believes that the results will be of interest to ITTC members, and they are presented here in anonymous form.

2.1 Turbulence Stimulation and Scaling

It was considered that the methods described in 7.5-01-01-01 may not reflect current practice. Members were asked which method(s) of turbulence stimulation they used, whether they were aware of the ITTC recommendations and when / whether they were adopted. Members were then asked to comment on situations in which ITTC recommendations were not adopted, and how the procedures might be improved. The final question in the first part related to the choice(s) of friction line for scaling.

Methods adopted are shown in Figure 2.1. Some facilities indicated that different approaches were used for different vessel types, and in some cases for different model materials. In particular several members commented on the need to adopt different techniques for vessels with large dynamic trim, and on appendages.

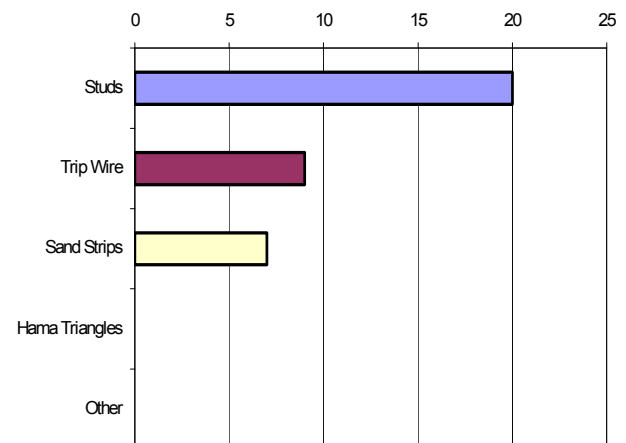


Figure 2.1 Turbulence stimulation method.

Results for compliance with ITTC procedure are shown in Figure 2.2. One reason given by some members for not adopting ITTC procedures was a reluctance to change their established practices without evidence of clear benefits in model-ship correlations. Additionally some members pointed out that clients sometimes specify the turbulence stimulation approach.

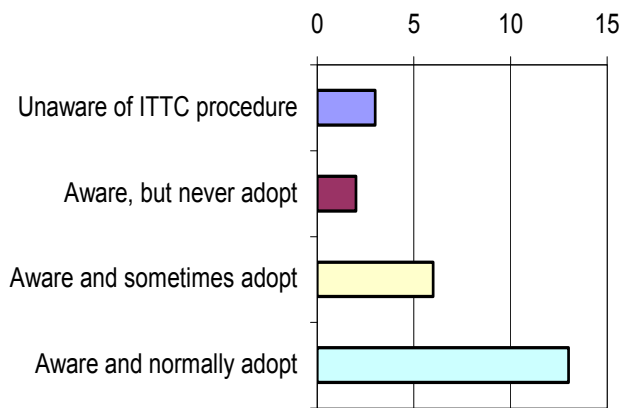


Figure 2.2 ITTC recommendations for turbulence stimulation method.

One issue raised by several members was the turbulence stimulation on bulbous bows, where current guidance was not considered satisfactory. An informal discussion with some of the members involved indicated that stimulation procedures for bulbous bows vary significantly between facilities. However, in order to propose improved procedures it is felt that both a detailed study of the phenomena involved, and a validation via model-ship correlation would be required. As a result no proposals have been made for modification of this procedure at this stage. Several members indicated that procedures were inappropriate for yachts.

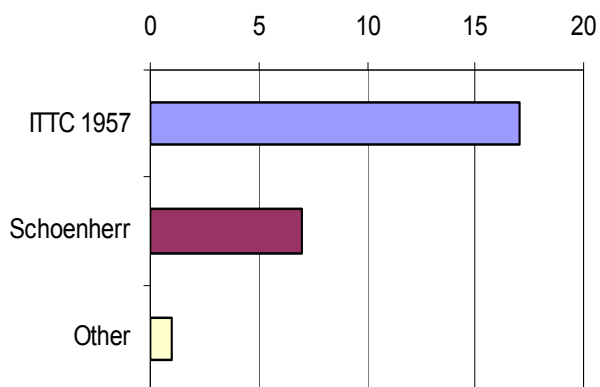


Figure 2.3 Friction line.

The results for the friction line are shown in Figure 2.3. Here there was a very clear (and expected) result; the Japanese members generally use the Schoenherr line, whilst all

others generally use the ITTC 1957 line; one member reported using the Prandtl-Schlichting approach in some cases.

2.2 Speed Measurement

The second part of the questionnaire related to the measurement of speed. It was felt that the existing procedure offered relatively little discussion of appropriate techniques for measuring speed given the importance of this measurement. Members were asked about the primary measurement system, the benchmark system used for calibration, the frequency of calibration and the accuracy of speed measurement.

Results showing primary and secondary measurement systems are given in Figures 2.4-2.5. It can be seen that a trailing wheel with an encoder or similar is the most popular primary method, though several members reported measuring speed directly from the carriage drive. Optical/proximity sensors are the most widely used secondary approach, whilst some facilities have custom-developed devices for speed calibration.

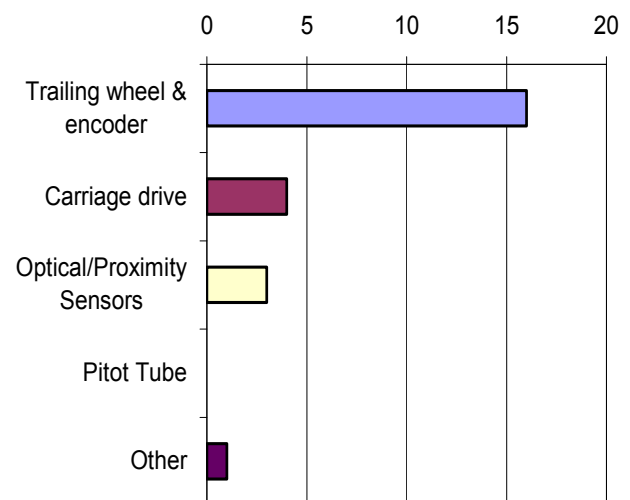


Figure 2.4 Primary speed measurement.

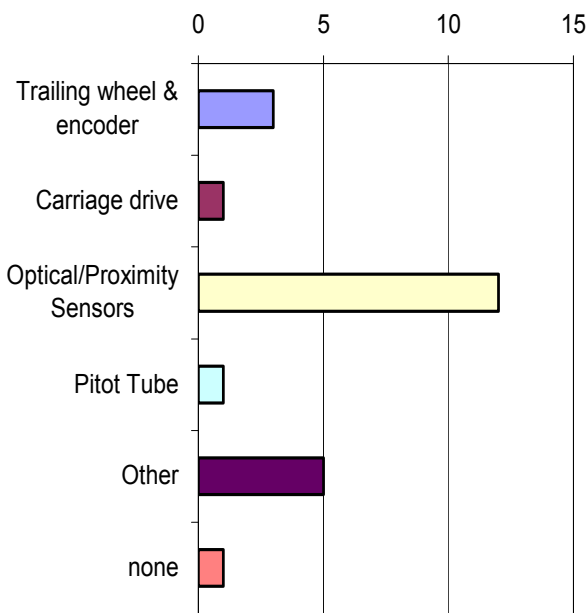


Figure 2.5 Secondary speed measurement.

Practice with regard to the frequency of calibration varied widely, between daily calibration and calibration over periods of several years. Whilst the reasons for this variation were not discussed, it may be dependant on the nature of the primary and secondary systems adopted. However the majority of replies indicated speed calibration once or twice per year.

All facilities reported that their speed measurement met the current standard (i.e. 0.1% of the maximum speed), and almost half of the members reported a considerably better accuracy (see Figure 2.6).

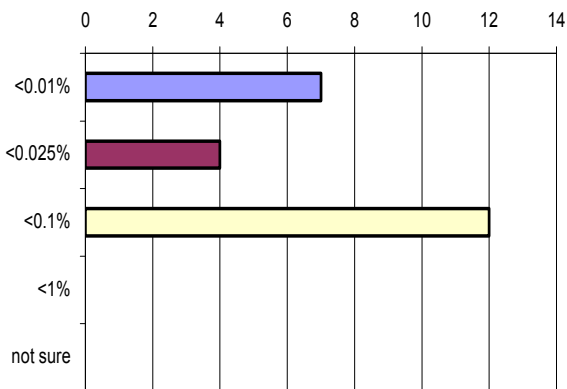


Figure 2.6 Speed measurement accuracy.

2.3 Model Installation

The final part of the questionnaire related to issues of model installation. The first question related to the part of the procedure related to the towing attachment. According to the procedure, the force should be applied “in the line of the propeller shaft and at the LCB in order to avoid artificial trim effects; however model should be attached to resistance dynamometer by a connection which can transmit and measure only a horizontal tow force”. Members were first asked if they normally followed this procedure. Results are shown in Figure 2.7.

The large majority of respondents indicated that they normally followed the procedure. One respondent who reported using an alternative practice pointed out the challenges associated with towing vessels with large shaft angles and/or large dynamic trim. Another indicated that in some cases (e.g. towing mathematical hulls, unconventionally propelled vessels) there is no defined shaft-line. It is clear that this procedure is not appropriate in such cases, and that an alternative strategy is required. It is suggested tentatively that towing at the waterline, using a connection providing only a horizontal force, may provide a reasonable alternative reference condition.

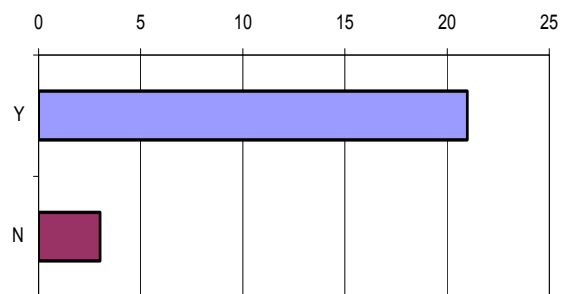


Figure 2.7 Compliance with installation procedure.

In cases in which the prescribed approach is impossible due to the geometry of the vessel, members were asked if they attempted to

correct the trim of the vessel. Results are shown in Figure 2.8.

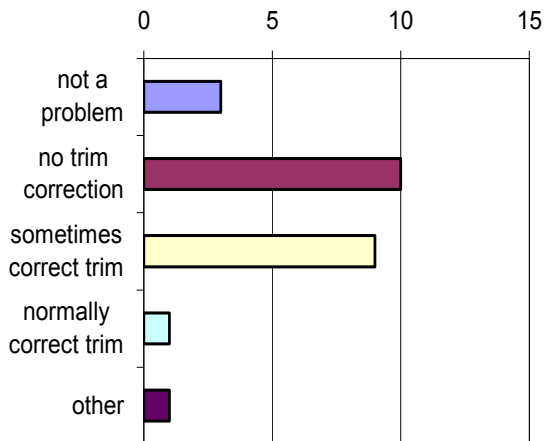


Figure 2.8 Trim correction approach.

Some members indicated that trim corrections were applied when vessels resistance were sensitive to trim and could adopt large dynamic trim, but not for conventional displacement vessels. A related question was asked with relation to practice adopted when vessels were not transversely stable. Results are shown in Figure 2.9.

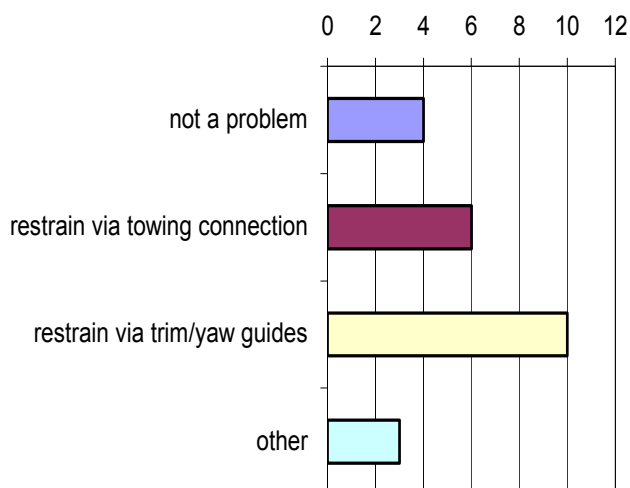


Figure 2.9 Transverse instability approach.

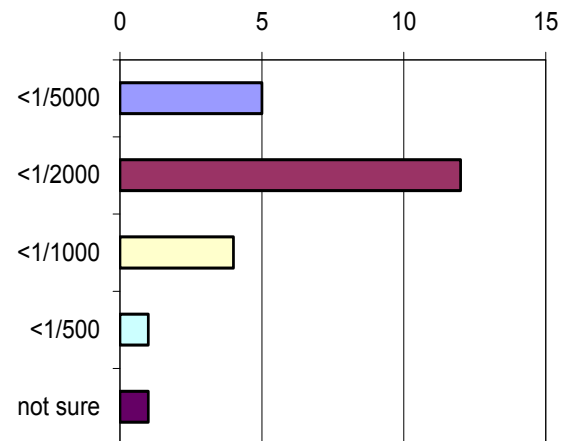


Figure 2.10 Alignment accuracy.

Finally, members were asked to comment on the approaches used to align the model in the tank, and the accuracy of alignment achieved. A range of approaches were adopted, with many using traditional approaches involving straight-edges and plumb-bobs, referenced to locations on the carriage. Other methods used included optical systems and measurement and minimisation of side force on the model. The reported accuracy of alignment achieved is shown in Figure 2.10.

These above results were used to inform of the proposed changes to the procedures.

2.4 New Facilities

As part of the RC questionnaire on test procedure, members were also asked to report any significant new facilities. Three responses were received:

Australian Maritime College. A new cavitation tunnel is being commissioned during 2008 at the Australian Maritime College. The tunnel is of the vertical plane, closed recirculating type. The drive system consists of a 6-bladed axial flow impeller and 14 bladed stator with AC variable frequency drive. The total motor power is 200kW at 1750rpm. The working section maximum velocity is 12m/s, and the maximum and minimum absolute

pressures are 400kPa, 4kPa. The cavitation number range is from 0.07 to 5.5.

Equipment and instrumentation includes propeller dynamometers, 6 component balances, water-jet test circuit, laser diagnostics, nuclei and incondensable gas injection and separation, working section boundary layer thickness control. The tunnel is designed for propellers or models of diameters from 150mm to 300mm.

The principal tests expected to be performed will be:

- 1) conventional cavitation testing.
- 2) cavitation nucleation and diffusion phenomena.
- 3) laser diagnostics.

CEHIPAR. CEHIPAR have installed a numerically-controlled five-axis milling machine with capacity to produce models and any other kind of work-pieces up to 10950 mm long, 2500 mm wide and 1200 mm high. The rotational speed can vary from 1000 to 20000 rpm. The total power is 12 kW. The machine can work with a range of materials including aluminium, bronze, wood, paraffin wax, PVC, polystyrenes, polyurethanes and other compounds.

Universities of Glasgow and Strathclyde. The Universities of Glasgow and Strathclyde have installed a new wavemaker in the Acre Rd Hydrodynamics Laboratory. The four-paddle absorbing wavemaker can move vertically in order to allow for different water depths. The wavemaker can generate periodic waves over frequencies from around 0.2Hz to 2 Hz. Periodic waves over 600mm in height can be generated; single breaking waves can be generated up to around 1000mm in height. The facility is designed for examination of highly non-linear unsteady phenomena such as survivability and capsizing in extreme seas.

3. TRENDS IN EXPERIMENTAL FLUID DYNAMICS

3.1 Introduction

This chapter reviews the recent research towards understanding physical meaning in hydrodynamics and applying new techniques in the area of experimental fluid dynamics (EFD). The trends in EFD related to the field of naval architecture is summarized into five parts: 1) new and advanced techniques in hydrodynamic experiments, 2) wake and pressure, 3) wave breaking and wave profile measurements, 4) full scale tests, and 5) drag reduction.

3.2 New and Advanced Techniques in Hydrodynamic Experiments

There have been remarkable developments in the hydrodynamic experiments and measurement techniques used in: a towing tank, a water tunnel, a water channel, a wind tunnel, and a wave tank. EFD progress has been closely related with the notable improvements of optical techniques such as: Particle Image Velocimetry (PIV), Particle Tracking Velocimetry (PTV), Laser Doppler Velocimetry (LDV), and Laser Induced Fluorescence (LIF), among others, and the ever-increasing computer power. The advanced techniques for hydrodynamic experiments are introduced and the recent research using these techniques is summarized.

Particle Image Velocimetry (PIV). PIV is an optical technique used to measure velocities and related properties in fluids. The fluid is seeded with particles which are generally assumed to faithfully follow the flow dynamics. The velocity field having 2 or 3 components is computed from the correlation between successive particle images using statistical methods.

The PIV technique is one of the most popular optical techniques to measure the

velocity field. Because it requires a relatively large space for CCD cameras, illuminating laser, computers, and other gear, its practical application has been limited in the naval hydrodynamic area. Recently, the PIV technique has been utilized to obtain the velocity field near a model ship in a towing tank overcoming this space limitation. Atsavapranee et al. (2004) measured the pressure, forces, and moments acting on a 5.27m submarine model, ONR Body-1 (bare hull, bare hull with sail and fully appended) and obtained the flow field including the vortical flow and flow separation near the model using PIV. Chen and Chang (2006) developed a flow velocity measurement system to observe velocity fields near ship models using a moving PIV system. These researchers discussed technical issues related to the application of PIV in towing tanks and suggested possible solutions for the problems caused in the moving PIV system. To remove the reflection of the laser light from cavitation, Foeth et al. (2006) utilized PIV measurement to investigate the cavitation developed on a hydrofoil surface with fluorescent tracer particles. Ryu et al. (2005) modified a PIV technique to obtain the flow field of the highly aerated area generated by wave breaking and greenwater since the highly aerated bubbly flow caused traditional PIV techniques to fail due to the uncontrollable scattering of the laser light. This modified PIV method, called bubble image velocimetry (BIV), was introduced by directly using bubbles as the tracer and measuring the bubble velocity by correlating the 'texture' of the bubble images.

Particle Tracking Velocimetry (PTV). PTV is also an optical technique to measure the fluid velocity including 2 or 3 components. While the PIV measurement computes one velocity vector from several particles in the interrogation area, PTV determines the velocity of each individual particle within the optical image.

Hoyer et al. (2005) presented an experimental setup and data processing

schemes for 3-D scanning PTV, which expands on the classical 3-D PTV through changes in the laser illumination and image acquisition and analysis. This technique allows for obtaining Lagrangian flow information directly from measured 3-D trajectories of individual particles. Lee et al. (2005) applied the adaptive hybrid two-frame PTV technique to measure the flow characteristics of a turbulent wake behind a marine propeller with five blades and compared the results to those obtained with PIV. This technique can be extended to investigate the nominal and effective wake distribution as well as the details of the flow field fore and aft of a rotating propeller behind a ship model.

Laser Induced Fluorescence (LIF). The LIF technique is a spectroscopic method used for studying structure of molecules, detection of selective species, and flow visualizations and measurements. The species in the fluid to be examined is excited with the help of a laser. The wavelength selected for the species and the fluorescence light is obtained by a camera with an optical bandwidth filter. This optical technique is often used to investigate the concentration and molecular behaviour in a fluid in combination with PIV or PTV.

Troy and Koseff (2005) presented the application of LIF for the generation and quantitative visualization of breaking progressive internal waves. LIF techniques can help in understanding the nature of turbulent and multi-phase flows due to wave breaking or cavitation phenomena.

Laser Doppler Velocimetry (LDV) and Acoustic Doppler Velocimetry (ADV). The LDV technique utilizes laser beams to intersect at a focal point, where they interfere and generate a set of straight fringes. The optical sensor is then aligned to the flow such that the fringes are perpendicular to the flow direction. As particles pass through the fringes, they reflect light with a doppler shift corresponding to the velocity of particles at the region of constructive interference into a photo detector.



The ADV technique employs a similar principle as LDV, but uses an acoustic wave instead of a laser beam. ADV sends out a beam of acoustic waves at a fixed frequency from a transmitter probe. These waves reflect off moving particulate matter in the water and three receiving probes obtain the change in frequency of the returned waves. These Doppler techniques are limited to measuring the fluid velocity at a point, but they can be employed to measure the fluid velocity near a wall and in full scale model tests with relatively high time resolution and the convenience of no calibration.

Cea et al. (2007) used ADV to measure the 3D instantaneous velocity of a highly turbulent free surface flow and applied several filters including the minimum/maximum threshold, the acceleration threshold, and the phase-space threshold in order to eliminate any corrupted velocity data.

Millward and Brown (2005) proposed a new method of measuring the actual wetted surface area of a model ship tested in a towing tank, which is based on capacitance where the model hull has been given a metallic coating and then an insulating coating so that it effectively becomes one plate of a capacitor with the water of a towing tank or a water channel becoming the other plate.

Song et al. (2007) conducted the resistance test of an ice breaker “Terry Fox” in a towing tank with synthetic ice whose data are compared with those conducted in the ice tank at IOT (Institute of Ocean Technology) Canada, showing a good correlation between the two data sets.

3.3 Wake and Pressure

The PIV technique is most frequently applied to measure the wake behind a structure or propulsion system. With the application of the PIV technique, Paik et al. (2007) studied the wake characteristics behind a marine

propeller with 4 blades at a high Reynolds number.

The PIV technique has also been employed to investigate cavitation. Wosnik et al. (2006) investigated the two phase flow structure in the wake of a 2-D hydrofoil (NACA0015) undergoing unsteady partial cavitation with time-resolved PIV, and to confirm the existence of the large-scale flow structure observed with Large Eddy Simulations (LES).

Using a stereoscopic PIV system, Perrin et al. (2007) investigated the flow structure near the wake zone of a circular cylinder including turbulence properties, of which the obtained flow was decomposed into the mean and fluctuating components by means of the phase-averaging method and the whole phase-averaged turbulent stress tensor was evaluated. In the wind tunnel, Jung et al. (2006b) investigated the three-dimensional velocity field of a prototype waterjet model, which extracted the dominant large scale flow structure and analyzed the turbulent characteristics using the proper orthogonal decomposition (POD). Perret et al. (2006) implemented a multiplane stereo PIV system to measure the three-component acceleration field in a plane of turbulent flows.

Felli and Felice (2005) utilized a LDV phase sampling technique to analyze the flow upstream and behind a four-blade, highly skewed installed propeller in the case of a twin-screw ship model in a large circulating water channel. This technique built the 3-D flow field with varying propeller angle in transversal planes located as close as possible to the blade trailing and leading edges.

Pressure Sensitive Paint (PSP) in a Wind Tunnel. PSP techniques allow global surface pressure measurements to be made using an optical detector. The surface is coated with PSP that is made up of a luminescent probe molecule held in an oxygen permeable binder. The probe molecule is chosen such that its luminescence is quenched by the oxygen. This

application is presently limited to wind tunnel use.

McGraw et al. (2006) employed a pressure sensitive paint to measure the dynamic and static surface pressure on a square cylinder, including vortex shedding, at three angles of incidence and a Reynolds number of 8.9×10^4 in a wind tunnel. From the phosphorescent oscillations, at the vortex shedding frequency, the time-dependent changes in pressure distribution were calculated. This technique can extend to dynamic systems where oscillating pressure changes are on the order of 230Pa and occur at frequencies in the range of 95–125Hz. Lee and Kang (2006) applied the PSP technique to measure the pressure distribution on a model surface at slow speeds in a wind tunnel. Four PSP formulations, each comprised of a porphyrin (PtOEP or PtTFPP) and a polymer (Poly(TMSP) or RTV-118), were tested and the performance of each combination was evaluated.

3.4 Wave Breaking and Wave Profile Measurements

Various experimental techniques have been applied to measure wave profiles and to understand wave kinematics including wave breaking phenomena. Karion et al. (2004) measured bow waves of two different bow geometries using a laser imaging technique at speeds ranging from 0.7 to 4.6m/s. Fluctuations on the free surface were quantified and characteristics of the breaking region were studied. Rice et al. (2004) applied various instruments (wave cut, finger probe, quantitative visualization) to obtain the near and far field wave pattern of a model ship and extended them to full scale measurements. Jung et al. (2005) and Jung et al. (2006a) used PIV in a 2-D wave tank to measure the velocity field in the vicinity of a rectangular floating structure in beam sea conditions. The mean velocity and turbulence properties are separated by a phase-averaging technique and the vortical flow fields due to the wave and

structure interaction were examined to understand the eddy making effect and the turbulence properties over one wave period. Stern et al. (2006b) implemented LDV and PIV to measure the flow field under a plunging breaking wave and to validate CFD results. Noblesse et al. (2006) investigated the bow wave generated by an immersed rectangular flat plate at constant speed along a straight course in calm water. Terrill and Taylor (2007) measured the full-scale wave field using LIDAR (Light Detection And Ranging) onboard the Sea Fighter.

3.5 Full Scale Tests

Sur and Chevalier (2004) performed full scale measurements of bow spray droplets created by the breaking bow wave for R/V Roger Revelle at speeds ranging from 1.0 to 7.7m/s and sea states of 0 to 3 using a high speed digital video camera. Starke et al. (2006) measured the full scale wake field using a ship-mounted LDV system during sea trials to validate computation results. Fu et al. (2006) carried out a sea trial test of the R/V Athena I to characterize: 1) the free surface in the bow region and behind the transom, 2) the spray in the bow region, 3) the air entrainment mechanisms and the bubble field around the boat, 4) the bubble dissolution times, and 5) visually document the free surface and the sub-surface bubble transport. In total, eleven separate instrumentation systems were deployed, as well as seven above water and three underwater camera systems. The sea trial test was performed with varying ship speeds of 6, 9, 10.5, and 12 knots, equivalent to Froude numbers based on length (47 m) of 0.14, 0.21, 0.24, and 0.29, respectively. The sea trial tests of a 294.6 tonne Catamaran, SEA FLYER, having a hydrofoil of 10 meter chord and 11 meter span, covered with polymer injection, showed that as much as 60 % reduction in the viscous drag component could be achieved, see Moore et al. (2006). Terrill and Taylor (2007) measured the full-scale wave field using



LIDAR (Light Detection And Ranging) onboard a naval surface ship (Sea Fighter).

3.6 Drag Reduction

The reduction of skin friction drag through turbulent boundary layer control has been of great interest from the viewpoint of energy efficiency since the late 90's. By the year 2005, the economic benefit of a 30% drag reduction in the ocean shipping industry was estimated to be 31 Billion US Dollars per year (Meng, 2005), which was based on \$50/barrel, half of today's oil price. There was a consensus to share the state-of-the-art research outcomes and a prospect toward the realization of drag reduction technologies between academia, research institutes and government agencies worldwide. Hence the 2nd International Symposium on Seawater Drag Reduction (ISSDR 2005) was held in Busan, Korea seven years after the 1st Symposium in Newport, Rhode Island, US. The symposium, jointly organized by US ONR (Office of Naval Research) and ASERC (Advanced Ship Engineering Research Center), Korea, witnessed the applicability of drag reduction strategies combined with novel experimental as well as theoretical analysis techniques. For those interested in the cutting-edge technology of drag reduction the proceedings of ISSDR 2005, with 57 papers by the pre-eminent researchers worldwide, is highly recommended. This report is based on the major research results reported in the proceedings and the subsequent journal publications from 2005 to 2007. For reviewing purposes on this issue, the paper of Joslin et al. (2005) is worth reading not only because it encompasses nearly the whole aspect of flow control, but also the unique perspective on the synergism of flow and noise control technologies relevant to both air and undersea vehicles is suggested.

Microbubble Injection. This technique is currently regarded as the most promising in terms of realization. The applicability of this method has been demonstrated from a full-

scale experiment on a 114-m training ship, SEIUN-MARU (Kodama et al., 2004a) and a 50m-long flat plate experiment (Kodama et al., 2004b).

In order to identify the drag reducing mechanism in more detail, a main issue of the research has been shifted to the deeper understanding of the drag-reducing mechanism by means of DNS (Direct Numerical Simulation) and PIV. Ferrante and Elgobashi (2005) investigated the effect of Reynolds number on the drag reducing efficacy of microbubbles in a turbulent boundary layer at $Re_0=1,430$ and $Re_0=2,900$ numerically. They showed that the increasing Reynolds number decreases the percentage of drag reduction. Kitagawa et al. (2005) demonstrated a novel experimental technique to visualize the interaction between the flow field and the microbubbles by means of PIV combined with a shadow image technique (SIT). Shen et al. (2006) made an assessment on the effect of bubble diameter on the drag reduction efficiency in a turbulent channel flow. The results indicate that the measured drag reduction by microbubbles is essentially independent of the size of the microbubbles over the size range tested ($18 \leq d^+ \leq 200$). The research by Kodama et al. (2006) showed that the drag reducing efficacy depends on the deformable character of bubbles, which is governed by Weber number. In case of less deformable (rigid) bubbles with $We = 50$, the local skin friction could increase. The research by Sanders et al. (2006) could be the most notable experimental endeavour to extend the Reynolds number, Re_x , to as much as 210 million, which is only one order less than that in real ship flows. They found that there are many different phenomena leading to the decrease of drag reduction efficiency in the previous results on low-Reynolds number flows. Murai et al. (2007) suggested the possibility of drag reduction using relatively large air bubbles, which is the intermediate case between the microbubble and air film conditions. Kunz et al. (2007) showed a comprehensive summary on the validation

status of a CFD tool development program for microbubble drag reduction predictions. An Eulerian two fluid model has been presented with specifics regarding physical models for interfacial dynamics, breakup, and coalescence.

Polymer Injection. Baik et al. (2005) shows how PIV techniques can be used to study changes in the configuration of the injected polymer and in the structure of the velocity field with increasing drag reduction. In Jovanović et al. (2006), turbulent drag reduction by dilute addition of high polymers is studied by considering local stretching of the molecular structure of a polymer by small scale turbulent motions in the region very close to the wall. The stretching process is assumed to restructure turbulence at small scales by forcing these to satisfy local axisymmetry with invariance under rotation about the axis aligned with the main flow. Deutsch et al. (2006) tested combined gas injection upstream of polymer injection. They reported higher levels of drag reduction than those obtained from the independent injection of polymer or microbubbles alone over a wide range of test conditions. These increased levels of drag reduction with combined injection were often greater than the product of the drag reductions obtained by the independent constituents, defined as synergy.

Moore et al. (2006) performed a sea trial test using the ONR technology demonstrator vessel, SEA FLYER, to characterize the performance of advanced polymer drag reduction.

Compliant Coatings. This could be the most classic and yet most controversial of the drag reduction technologies. Bandyopadhyay et al. (2005) reported the experimental results from a collaborative effort between the USA, Russia, and UK on the development of compliant coatings for undersea application to the reduction of drag. The focus was on the "shelf-life" of coatings. They showed that, with some exceptions, drag reduction generally deteriorates with the age of the coatings.

Active Control. There have been many theoretical researches on feedback and (sub)optimal control to demonstrate an upper bound for the drag reducing capabilities in ideally arranged situations. Min et al. (2006) showed the exemplary result that skin-friction drag can be sustained below that corresponding to the laminar profile when the flow is subjected to surface blowing and suction in the form of an upstream travelling wave. A key mechanism that induces the sublaminal drag is the creation of negative Reynolds shear stress in the wall region, where normally positive Reynolds shear stress is expected given the mean shear. In their latest review paper, Kim and Bewley (2007) introduced the essential ingredients of linear systems and control theory to the fluid mechanics community, to discuss the relevance of this theory to important open problems in the optimization, control, and forecasting of practical flow systems of engineering interest, and to outline some of the key ideas that have been put forward to make this connection tractable.

3.7 Conclusions

Experimental techniques and analysis methods have significantly progressed in EFD for velocity measurement, wave breaking and profile measurement, full scale tests, and drag reduction technology. Optical techniques have been extensively utilized to obtain the wake field and turbulence flow. The PIV technique has been recently applied to measure the flow field near a model ship in a towing tank, which can provide detailed velocity profiles near the model ship helping to validate CFD results. The limitation of PIV and PTV techniques, such as light saturation at the aerial area, can be overcome by the combination with LIF, which can improve research in small scale flows.

Although point measurements are limited, Doppler techniques (LDV and ADV) can be employed to measure the fluid velocity near the wall for full scale and model scale tests with relatively high time resolution and the

convenience of no calibration. The ADV technique is especially easily employed to measure the velocity in full scale tests without calibration and relatively little expense. Various experimental techniques (laser imaging, wave cut, finger probe, quantitative visualization, LIDAR) have been applied to measure wave profiles and wave breaking patterns and optical techniques such as PIV and LDV have been utilized to study the wave kinematics. Experiments at full scale are increasing in order to develop and verify methods for predicting the full-scale performance of marine structures from model scale tests. Recently, extensive full scale investigations related to maneuvering and speed to study bubble effects and polymer injection to reduce the drag on ships have been carried out.

4. SCALING AND EXTRAPOLATION METHODS

The speed-power prediction is one of the most important functions of towing-tank facilities. ITTC's recommended procedure for power estimation is based on the full-scale resistance, which is very difficult to measure and data is seldom available. Instead of full-scale resistance measurements the extrapolation of model-scale resistance to full-scale resistance is usually used. During the procedure, the friction line plays a major role to predict both model- and full-scale friction resistances. The 25th ITTC RC conducted analytical studies of friction lines, aiming at a possible recommendation for a new formula. The basic discussion is provided by the recent work of Katsui et al. (2005). In the following, an overview is given of the study.

4.1 Introduction

Recent computer developments enable the calculation of ship viscous flows at full scale Reynolds numbers. However, it is difficult to verify the calculated flow for full scale

Reynolds numbers, since the available experimental data is quite rare. Empirical equations for frictional resistance, such as Schoenherr's formula (Schoenherr, 1932) and the ITTC'57 correlation line, are often used for the verification, although these formulae do not account for experimental data at full scale Reynolds number. In fact, recent reliable measurements of friction resistance for a flat plate indicate that Schoenherr's formula overestimates the local frictional coefficient by 2-3% even in the range of model scale Reynolds numbers. Hence, more precise re-evaluation of frictional resistance is necessary, covering a wide range of Reynolds number from model-scale to full-scale ship flows.

In the present report, the flat plate friction coefficient is evaluated by solving differential equations composed of the momentum integral equation and Coles' wall-wake law. The latter gives the velocity distribution in a turbulent boundary layer. The model parameters in Coles' law are determined based on the latest reliable experimental data obtained by Osaka et al. (1996), so that Coles' law gives a more accurate velocity distribution that is expected to yield a more correct friction coefficient. The results obtained for the flat plate friction coefficient, local friction coefficient and velocity distribution in the boundary layer are compared with experimental data. Grigson (1993) performed a similar study by solving the momentum integral equation, and it appears that there are considerable differences in the results between the present and Grigson's methods. These differences in the results are also carefully examined.

4.2 Method to Calculate Friction Coefficient

Momentum Integral Equation. The flat plate friction coefficient can be given by the solution to the momentum integral equation. For a two dimensional flat plate flow without pressure gradient, the momentum integral equation is expressed as follows:

$$\frac{d\theta}{dx} = \frac{1}{2} C_f \quad (4.1)$$

Integrating this equation from the leading edge of the flat plate, we obtain the relation between the momentum thickness and the friction coefficient.

$$\theta = \frac{1}{2} C_f x \quad (4.2)$$

The ratio of momentum thickness to boundary layer thickness is expressed with non-dimensional values as follows.

$$\frac{\theta}{\delta} = \frac{1}{2} C_f \frac{R_n \sigma}{\delta^+} \quad (4.3)$$

Where, definition of momentum thickness is

$$\theta \equiv \int_0^{\delta} \frac{u}{U} \left(1 - \frac{u}{U}\right) dy \quad (4.4)$$

By using the non-dimensional value based on frictional velocity, the ratio of momentum thickness to boundary layer thickness is as follows.

$$\frac{\theta}{\delta} = \frac{1}{\delta^+} \int_0^{\delta^+} \sigma u^+ (1 - \sigma u^+) dy^+ \quad (4.5)$$

Hence, Eq. 4.3 through Eq. 4.5 yield a relation between the velocity profile in a turbulent boundary layer and the frictional coefficient, which is given by

$$\int_0^{\delta^+} u^+ (1 - \sigma u^+) dy^+ = \frac{1}{2} C_f R_n \quad (4.6)$$

The normalized friction velocity σ used in the above equation is expressed with the local frictional coefficient C_f , i.e.,

$$\sigma \equiv \frac{u_\tau}{U} = \sqrt{\frac{C_f}{2}} \quad (4.7)$$

Eq. 4.1 and Eq. 4.2 lead to a relation between the frictional coefficient and the local frictional coefficient as follows:

$$C_f = C_F + \frac{dC_F}{dx} = C_F + R_n \frac{dC_F}{dR_n} \quad (4.8)$$

Therefore, the normalized frictional velocity is given as

$$\sigma = \sqrt{\frac{C_F + R_n \frac{dC_F}{dR_n}}{2}} \quad (4.9)$$

Along with additional information, i.e., the velocity distribution in the turbulent boundary layer, Eq. 4.6 and Eq. 4.9 yield a differential equation to solve for the frictional coefficient.

Velocity Profile in a Turbulent Boundary Layer. It is well known that the velocity distribution of a turbulent boundary layer for a flat plate flow without pressure gradient has a similarity law based on the frictional velocity. As shown in Fig. 4.1, a turbulent boundary layer is divided into three regions.

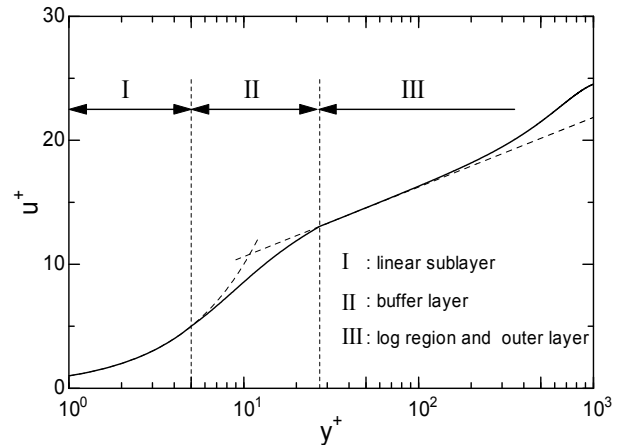


Figure 4.1-Time averaged structure of turbulent boundary layer (I.- Linear sublayer, II- Buffer layer, III- Log region and outer layer).

In the linear sublayer, the viscous stress is dominant and the velocity distribution is proportional to the distance from wall. On the other hand, in the log region and outer layer, the Reynolds stress is dominant. In the intermediate region between them, i.e., buffer layer, viscous stresses and Reynolds stresses



are at the same level. In each region, the velocity distribution is represented as follows.

$$\text{I. } u^+ = y^+ \quad (4.10)$$

$$\text{II. } \frac{du^+}{dy^+} = \frac{1}{1 + v_i/v} \quad (4.11)$$

$$\frac{v_i}{v} = \kappa(y^+ - \lambda_1 \tanh(y^+ / \delta^+)), \quad \lambda_1 = 11$$

$$\text{III. } u^+ = \frac{1}{\kappa} \ln(y^+) + C + \frac{\Pi}{\kappa} w(y^+ / \delta^+) \quad (4.12)$$

$$w(y^+ / \delta^+) = 1 - \cos(\pi y^+ / \delta^+)$$

Eq. 4.11 and Eq. 4.12 are Reichardt's equation and Coles' wall-wake law (Coles, 1987), respectively. The parameters used in Coles' law, κ , C and Π are Kármán's constant, the intercept constant of the log law and the wake parameter, respectively, and the values are determined by using experimental data. Indeed, the parameters have a large influence on the friction coefficient, because Coles' law covers quite a wide range except for the near wall region. Therefore, accuracy in the parameters is a key issue for correct prediction of friction coefficient.

Osaka et al. (1996) investigated the flow structure around a flat plate without pressure gradient, and emphasized that uniformity of flow in the crosswise direction is crucial for accurate measurement of flat plate friction resistance. The measured local friction resistance (obtained with a shear stress meter) is lower than that from Schoenherr's formula, and they believe that this is due to more uniformity of flow in the crosswise direction in their measurements. The measurements were performed for $Rn_\theta = 840 \sim 6220$ (i.e., assumedly $Rn = 2.8 \times 10^5 \sim 3.5 \times 10^6$). Based on their investigations, the following conclusions were made:

(i) The velocity distribution in a turbulent boundary layer indicates a logarithmic region

in the Reynolds number range considered in the study, and the Kármán constant κ is 0.41.

(ii) The intercept constant of the log law, C , is about 5.0.

(iii) The wake parameter follows Eq. 4.13 by Coles (1987) and approaches 0.62 at high Reynolds number.

$$\Pi = 0.62 - 1.21 \exp(-\delta^+ / 290) \quad (4.13)$$

Although Osaka's experiment is in the range of model scale Reynolds numbers, it is unlikely that flow structure drastically changes at high Reynolds number. Hence, we use $\kappa = 0.41$, $C = 5.0$ and Eq. 4.13 for the wake parameter. Then, integration of Eqs. 4.10 through 4.12 yields the momentum thickness.

Differential Equation to Solve Friction Coefficient. Now, we define the functions F_1 and F_2 as follows.

$$\begin{aligned} F_1(\delta^+) &\equiv \int_0^{\delta^+} u^+ dy^+ \\ &= \int_0^{y_1^+} y^+ dy^+ \\ &+ \int_{y_1^+}^{y_2^+} \left(\int_{y_1^+}^{y^+} \frac{dy^+}{1 + \kappa(y^+ - \lambda_1 \tanh(y^+ / \lambda_1))} + y_1^+ \right) dy^+ \\ &+ \int_{y_2^+}^{\delta^+} \left(\frac{1}{\kappa} \ln(y^+) + C + \frac{\Pi}{\kappa} \left(1 - \cos\left(\pi \frac{y^+}{\delta^+}\right) \right) \right) dy^+ \end{aligned} \quad (4.14)$$

$$\begin{aligned} F_2(\delta^+) &\equiv \int_0^{\delta^+} (u^+)^2 dy^+ \\ &= \int_0^{y_1^+} (y^+)^2 dy^+ \\ &+ \int_{y_1^+}^{y_2^+} \left(\int_{y_1^+}^{y^+} \frac{dy^+}{1 + \kappa(y^+ - \lambda_1 \tanh(y^+ / \lambda_1))} + y_1^+ \right)^2 dy^+ \\ &+ \int_{y_2^+}^{\delta^+} \left(\frac{1}{\kappa} \ln(y^+) + C + \frac{\Pi}{\kappa} \left(1 - \cos\left(\pi \frac{y^+}{\delta^+}\right) \right) \right)^2 dy^+ \end{aligned} \quad (4.15)$$

where

$$y_1^+ = 5.0, y_2^+ = 27.2, \lambda_1 = 11,$$

$$\kappa = 0.41, C = 5.0$$

$$\Pi = 0.62 - 1.21 \exp(-\delta^+ / 290)$$

With these two functions, Eq. 4.6 is given by

$$F_1(\delta^+) - \sqrt{\frac{C_F + Rn \frac{dC_F}{dRn}}{2}} F_2(\delta^+) = \frac{1}{2} C_F Rn \quad (4.16)$$

Considering that the velocity at the edge of the boundary layer is equal to the uniform flow velocity, we have an equation for δ^+ as follows:

$$\frac{1}{\sigma} = \frac{1}{\kappa} \ln(\delta^+) + C + \frac{\Pi}{\kappa} w(1) \quad (4.17)$$

which yields the following:

$$\sqrt{\frac{2}{C_F + Rn \frac{dC_F}{dRn}}} = \frac{1}{\kappa} \ln(\delta^+) + C + \frac{2}{\kappa} (0.62 - 1.21 \exp(\delta^+/290)) \quad (4.18)$$

Hence, starting with $Rn=10^4$ and a guessed $C_F(Rn=10^4)$, e.g., value given by Schoenherr's formula, we solve Eqs. 4.16 and 4.18 by using Newton's method for dC_F/dRn and δ^+ . Then, dC_F/dRn is integrated using a Runge-Kutta scheme to get C_F for $Rn+\Delta$, where Δ is the increment of Rn in the integration. The above procedure is repeated until Rn reaches 10^{10} . It is noteworthy that C_F for $Rn>10^6$ converges to the same value although different $C_F(Rn=10^4)$ is used, which is due to the parabolic nature of the present equation system.

4.3 Results and Comparison with Experiments

Velocity Distribution in a Boundary Layer.

Solution to Eqs. 4.16 and 4.18 yields δ^+ , which gives the boundary layer thickness and wake parameter Π . By using the values, the velocity distribution in the boundary layer at each

Reynolds number is given by Eqs. 4.10 through 4.12. Fig. 4.2 shows a comparison of the present results with Osaka et al.'s measurements. The Reynolds number used in Fig. 4.2 is based on the momentum thickness ($Rn_\theta = U\theta/\nu$), $Rn_\theta = 840, 1230, 2100, 2990, 4400, 5230, 6040$, which correspond to $Rn = 2.77 \times 10^5, 4.58 \times 10^5, 9.22 \times 10^5, 1.45 \times 10^6, 2.36 \times 10^6, 2.93 \times 10^6, 3.50 \times 10^6$ in the present calculation, respectively. The present results agree well with the measurements.

Local Friction Coefficient. Fig. 4.3 shows a comparison of the local friction coefficient. The white circles are the measurements of Osaka et al. and the chain double-dashed line is the present calculation. Osaka et al.'s measurements indicate lower values than those from Schoenherr's formula as well as other previous experiments, which were performed for model ship scale Reynolds numbers. Osaka et al. claimed that, for these previous experiments, the uniformity of flow in the crosswise direction might not be as satisfactory as that for their experiments. It is noteworthy that the present calculations show very close agreement with Osaka et al.'s measurements.

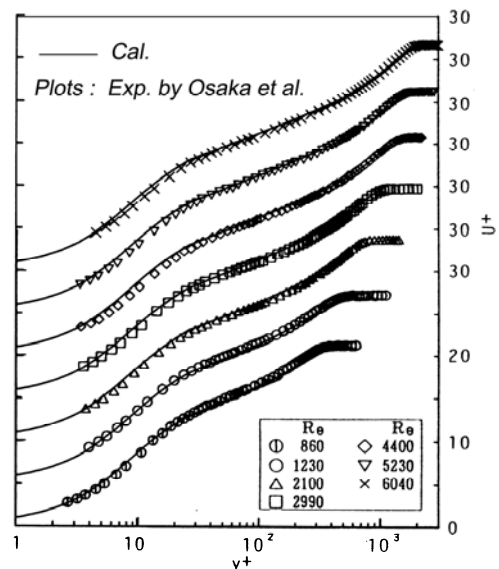


Figure 4.2 Comparison of velocity profiles in a turbulent boundary layer. Experimental results are obtained by Osaka et al. (1996).

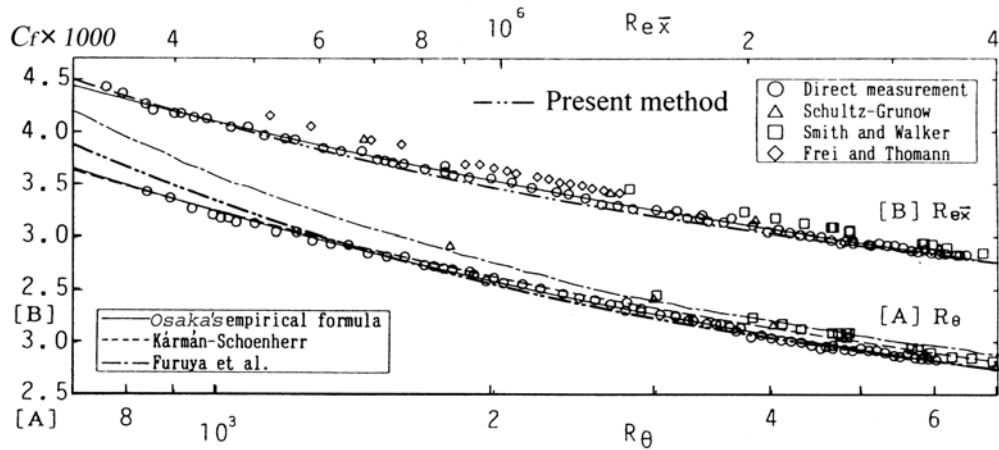


Figure 4.3 Comparison of local friction coefficient. (Exp. - Osaka et al., 1996)

4.4 Comparison with Grigson's Method

As mentioned, Grigson (1993) also performed a similar investigation on the flat-plate frictional resistance, based on the solution to the momentum-integral equation and Coles' wall-wake law. The present method differs from Grigson's regarding two major aspects, i.e., the numerical procedure and the values of parameters used in Coles' law. In Grigson's method, the numerical calculation is carried out based on Eq. 4.1, and the effect of the derivative of wake parameter ($\partial\Pi/\partial Rn$) is neglected. In the present method, the numerical calculation is carried out based on Eq. 4.2 and the $\partial\Pi/\partial Rn$ term is included, and fewer approximations are made.

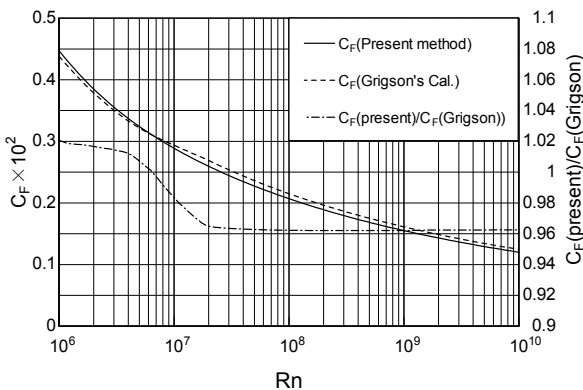


Figure 4.4 Comparison of flat-plate frictional resistance coefficient with Grigson's method.

Grigson used $\kappa=0.419$, $C=5.5$ in Coles' law, and determined the wake parameter Π from Smith and Walker's experiments (Smith and Walker, 1959). The present method uses $\kappa=0.41$, $C=5.0$ and determined Π from Eq. 4.13. Fig. 4.4 shows a comparison of the flat-plate frictional resistance coefficient C_F between the present and Grigson's methods. There are considerable differences between the two both at model-scale and full-scale Reynolds numbers. In order to investigate the cause of the differences, further calculations are made with particular focus on the influence of the parameter in Coles' law on the results.

Fig. 4.5 shows comparison of C_F between the present and Grigson's methods, while for both methods, the same parameters in the Coles' law as those for the present method are used. The differences are obvious in the region of $Rn < 10^7$. As shown in Fig.4.6, the wake parameter Π indicates rapid change in the region, therefore the derivative of Π must be included in the calculation as is done for the present method. On the other hand, for higher Reynolds number, the differences of C_F are not significant. This implies that, for the region, another element must be considered to investigate the cause of the aforementioned differences between the two methods, i.e., assumptions made on the wake parameter Π .

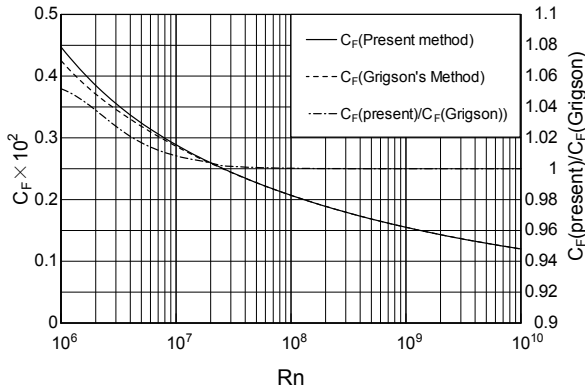


Figure 4.5 Comparison of flat-plate frictional resistance coefficient with Grigson's method. Parameters in the Coles' law are set to the same values in both methods.

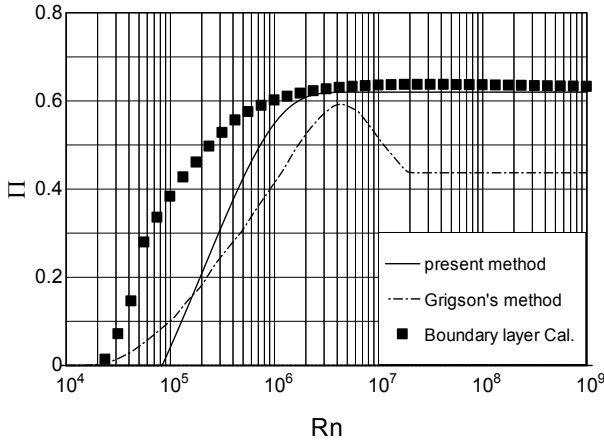


Figure 4.6 The behaviour of wake parameter corresponding to Reynolds number.

In Fig. 4.6, Π in both methods is compared. Large differences are seen in the high Reynolds number region. In order to judge the validity of the results, in the present study, further numerical calculations of the turbulent boundary equation were performed. The details are described below.

4.5 Numerical Calculation of Boundary Layer Equation

In order to investigate the mean flow structure in the outer region of a turbulent boundary layer at high Reynolds numbers, the turbulent boundary layer equation is solved with the Cebeci-Smith turbulence model.

Basic Equations. The basic equations are the steady turbulent boundary layer and continuity equations.

$$u \frac{\partial u}{\partial x} + v \frac{\partial u}{\partial y} = \frac{\partial}{\partial y} \left(\nu_e \frac{\partial u}{\partial y} \right) \quad (4.19)$$

$$\frac{\partial u}{\partial x} + \frac{\partial v}{\partial y} = 0 \quad (4.20)$$

Where ν_e is effective viscosity given by

$$\nu_e \equiv 1 / Rn + \nu_t / (UL) \quad (4.21)$$

By using the similarity variable η and the normalized stream function f defined as

$$\eta \equiv \sqrt{Rn/x} \cdot y \quad (4.22)$$

$$f \equiv \sqrt{Rn/x} \cdot \psi \quad (4.23)$$

the basic equations are transformed to the following form:

$$Rn \frac{\partial}{\partial \eta} (\nu_e \cdot v) + \frac{1}{2} f \cdot v = x \left(u \frac{\partial u}{\partial x} - v \frac{\partial f}{\partial x} \right) \quad (4.24)$$

with u and v defined as

$$u \equiv \frac{\partial f}{\partial \eta}, \quad v \equiv \frac{\partial u}{\partial \eta} \quad (4.25)$$

The above equation is solved with the Cebeci-Smith turbulence model, which gives the eddy viscosity for inner and outer regions as follows.

$$\nu_{ii} = \sqrt{\frac{x}{Rn}} \kappa^2 \eta^2 \left(1 - \exp\left(-\frac{y^+}{26}\right) \right) |v| \quad (4.26)$$

$$y^+ = (Rn \cdot x)^{\frac{1}{4}} \sqrt{v(0)} \eta \quad (4.27)$$

$$\nu_{io} = 0.0168 \sqrt{\frac{x}{Rn}} (\eta_{\max} - f_{\max})^2 \left(1 + 5.5 \left(\frac{\eta}{\eta_{\delta}} \right)^6 \right)^{-1} \quad (4.28)$$

where η_{\max} and f_{\max} are the values of η and f at the boundary layer edge. η_{δ} is the boundary layer thickness in the η coordinate.

Computational Conditions. The calculation is carried out in the range of $Rn=10^4 \sim Rn=10^9$ with Keller's box scheme (Cebeci, 2004). The range of η is $0 \leq \eta \leq 320$, which is discretized using 1,000 points; and the stream wise range is $0 \leq x \leq 1$, which is discretized using 20,000 points. The minimum grid spacing in the η direction is 1.0×10^{-5} , which corresponds to a grid spacing of 3.16×10^{-10} in the physical coordinate y direction at $Rn=10^9$. The Blasius solutions are used to provide initial values at $Rn=10^4$.

Results of Wake Parameter Behaviour at High Reynolds Number. Fig. 4.6 shows the wake parameter Π obtained from solutions to the above-described boundary layer equation. As shown in the figure, the computed Π indicates closer agreement with that used in the present method (which is derived from Eq. 4.13), while that used in Grigson's method indicate significant differences from the results, regarding magnitudes as well as trends. This result clearly supports the validity of using Eq. 4.13 for estimation of the wake parameter for the full-scale ship Reynolds number region.

4.6 Simple Formula to Estimate Flat-Plate Friction Coefficient

For convenience, a simple formula that approximately represents the flat-plate frictional resistance coefficients obtained by the present method is considered. A similar form as that of the ITTC '57 line is used, i.e.,

$$C_F = A / (\log Rn - D)^{B \log Rn + C} \quad (4.29)$$

The model constants A , B , C and D are determined from a least-square method to represent the results from the present method, and finally the following formula is obtained:

$$C_F = \frac{0.0066577}{(\log Rn - 4.3762)^{0.042612 \cdot \log Rn + 0.56725}} \quad (4.30)$$

This formula is applicable in the range of $1.0 \times 10^6 \leq Rn \leq 7.0 \times 10^9$, and gives the frictional coefficient within 0.1% error from the numerical results from the present method.

Lastly, the comparison of flat-plate frictional resistance coefficient with Schoenherr's, ITTC '57 and Hughes' formulae (Hughes, 1952) is shown in Fig. 4.7.

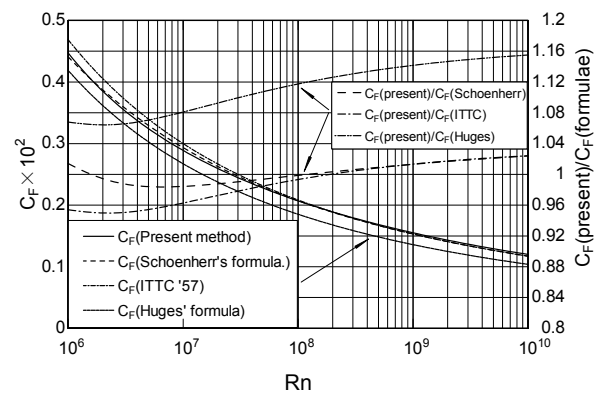


Figure 4.7 Comparison of flat-plate frictional resistance coefficient with empirical formulae.

4.7 Concluding Remarks

The 25th ITTC RC conducted an analytical study on friction lines, aiming at possible recommendation for a new formula. A formula proposed by Katsui et al. (2005) is based on the solution of an exact differential equation for the momentum-integral equation and Coles' wall-wake law. Comparison of results with that of Grigson (1993) indicates that there are considerable differences in the friction coefficient between the two methods for both model-scale and full-scale Reynolds numbers, e.g., as compared to Grigson's values, that are about +2%, -2%, and -4% for $Rn=10^6$, $Rn=10^7$, and $Rn=10^9$, respectively.

The method of Katsui et al. (2005) differs from that of Grigson (1993) regarding: (i) the latest experimental results (Osaka et al., 1993) are considered; (ii) a more exact form of the

differential equations is solved; and (iii) the derivative of the wake parameter is included in the calculation, that appeared to yield a significant difference of results at model-scale Reynolds numbers. Katsui et al. (2005) particularly noted that the differences between the two methods in model- and ship-scale Reynolds number are attributed to the derivative term of the wake parameter, and the wake parameter itself, respectively.

A formula proposed by Katsui et al. (2005) will be useful for verification of CFD results at ship-scale Reynolds numbers, and in fact, development of such a friction formula was a main objective of their work. On the other hand, results presented in their work along with theoretical considerations will need further discussion before proposing a new friction line.

4.8 Nomenclature for Chapter 4

x, y	Coordinates of stream and vertical direction
U	Flow velocity of uniform flow
L	Plate length
u	Flow velocity of x direction
ρ	Fluid density
ν	Viscosity
ν_t	Eddy viscosity
τ_w	Friction stress at wall
u_τ	Friction velocity
δ	Boundary layer thickness
θ	Momentum thickness
C_f	Local friction coefficient
C_F	Flat plate friction coefficient
Rn	Reynolds number based on the flat plate length ($= UL/\nu$)
Rn_θ	Reynolds number based on momentum thickness ($= U\theta/\nu$)
u^+	Velocity of x direction normalized by friction velocity ($= u/u_\tau$)

y^+	Reynolds number based on friction velocity and distance from wall ($= u_\tau y/\nu$)
δ^+	Reynolds number based on friction velocity and boundary layer thickness ($= u_\tau \delta/\nu$)
σ	Normalized friction velocity ($= u_\tau/U$)
κ	Kármán's constant
C	Intercept constant of log law
Π	Wake parameter

5. TRENDS IN COMPUTATIONAL FLUID DYNAMICS

5.1 Introduction

This chapter summarizes the ongoing research effort toward the development of efficient numerical tools in the area of computational hydrodynamic analysis and design of ships, reporting trends in research and experience in industrial applications as emerged from the literature of the last three years. The section opens with some practical applications of CFD, followed by progress in computational methods that have evolved over the last three years, and new application areas that are being pursued.

5.2 Practical Applications of CFD

Numerous computational predictions for ship flows at model and full scale are appearing in the literature. There have been demonstrations of inviscid predictions for decades and demonstrations with the Reynolds Averaged Navier-Stokes (RANS) equations have also become routine. All of these efforts cannot be covered in the current report, but an effort is made to highlight the progress and different approaches being pursued by the community in this and the subsequent sections.



Inviscid Flow Calculations. Inviscid calculations are routinely done for many ship types and by many organizations. One new development in this area is the work of Noblesse and Yang (2006) and their development of the Neumann-Michell potential flow model for the steady free surface flow about a ship. The authors argue the classical Neumann-Kelvin model is not a consistent linear flow model, but the Neumann-Michell model is. The model also does not require the solution of a line integral around the ship waterline and is solved iteratively exploiting the slenderness of ship forms. Demonstrations have been made for a Wigley and series 60 hulls as well as a trimaran in Yang, Kim and Noblesse (2007).

Viscous Flow Computations at Model Scale. Model scale computations are largely discussed in the subsequent sections as they relate to various methods and new application areas. A comparison of resistance at model scale for the R/V Athena, a high speed monohulls, by four separate groups, utilizing five CFD codes was discussed by Wilson et al. (2006). All together, seven separate solution sets were submitted and compared to model test data of wave field measurements and the total resistance for two different ship speeds. All of the CFD predictions were performed in a “blind” manner, with the computational results provided prior to the experimental measurements being released. Comparisons were also made between the different solution methods, along with discussion of the particular grid generation methods, numerical solution techniques, ease of use, and computational expense to generate the solutions. These comparisons are provided together to assess computational methods for predicting the wave fields generated by surface ships, including wave breaking. It was found that each of the different solution methods has different advantages and disadvantages, and each has certain specific requirements for obtaining accurate solutions of a surface ship wave field.

Mixed Viscous/Inviscid Calculations. There continue also to be mixed approaches using a combination of inviscid and viscous methods. Huan and Huang (2007) combined a nonlinear free surface potential flow solver with a RANS solver, for the viscous contribution, with the free surface specified with the potential flow solver. In their examples the potential flow solver can handle either a wet or dry transom.

Viscous Flow Computations at Full Scale. There is continued interest in making full scale predictions with RANS codes. Bhushan et al. (2007) demonstrate predictions for the Athena, with both RANS and Detached Eddy Simulation (DES). The authors use wall-functions with and without surface roughness for the computations. Full scale powering predictions are compared with experimental data for RPM and additional comparisons are made with a full scale towed configuration, which was free to sink and trim. Significant differences were seen in the computations with the rough wall predictions generally comparing better with the experimental data than the smooth wall predictions.

The EFFORT (European Full-scale FLOW Research and Technology) project, which ran from 2001 to 2005 as a EU-sponsored programme was a cooperation between several European institutes, universities and industrial sponsors. The aim of the project was to provide validated full-scale CFD tools and to introduce these tools to industry. The EFFORT project has involved extensive validation studies for a variety of vessels, both at model and full scale, including a geometrically complex twin-screw hopper dredger. Papers have shown that accurate viscous flow computations are possible at full scale and show good correlation with experimental data measured during the sea trials with ship mounted LDV systems. Starke et al. (2006) presented validations for a full-block tanker, a container vessel, a research vessel and the twin-screw hopper dredger. Regnstrom and Bathfield (2006) and

Visonneau et al. (2006) also show good comparisons for the frigate and hopper dredger. These studies show the importance of turbulence modeling even at full scale. The importance of grid resolution and the difficulty of obtaining grid independent solutions, particularly around shafts and struts, for the more complicated configuration, is also discussed.

5.3 Progress in Viscous Flow Calculation Methods

Free Surface Treatment. Capturing methods have become routine, and even standard, for many RANS free surface predictions. Single phase level set and volume of fluid methods have been demonstrated to handle steep and breaking waves. With the single phase level set methods only the water is computed and the methods can provide a sharp interface and still be quite robust. Single phase level set methods have been used by many groups for a variety of ship flows related to resistance predictions (e.g. Di Mascio et al., 2007; Wilson et al., 2007a) as have multi-phase methods (e.g. Maki et al., 2007; Visonneau et al., 2006) to name but a few. Two-phase level set techniques that solve for both the air and water are also being considered by some groups for ship problems (e.g. Stern et al., 2006b). With all of these methods the accuracy of the free surface prediction is directly dependent on the grid resolution near the free surface. Queutey and Visonneau (2007) discuss the importance of the discretisation scheme used for solving the transport equations near the free surface interface in order to get a good representation of the free surface, even with fine grids. The Constrained Interpolation Profile (CIP) method also continues to be used by various groups for capturing the free surface and Takizawa et al. (2007) recently demonstrated the method for ship flows, but not directly for resistance related predictions.

Grid Types. Gridding is an issue for CFD and grid options continue to evolve.

Immersed boundary methods can greatly simplify the grid generation process. With these methods grids are generated, often Cartesian, that do not conform to the geometry. Consequently, gridding is often trivial, but the solution needs to account for the geometry within the solution domain. A recent review of immersed boundary methods was given by Mittal and Iaccarino (2005). For ship flows Dommermuth et al. (2006, 2007) is using Cartesian grids with the volume of fluid method to reproduce breaking waves around ships and the resulting forces. Only a paneling of the surface is required to define the immersed boundary representation of the geometry on a Cartesian grid. The free surface is predicted with a high degree of detail using grids on the order of 20 to 30 million points. However, viscous effects are not directly computed and frictional resistance is estimated with the ITTC friction line. Yang et al. (2007) uses a combination of Cartesian grids and immersed boundary conditions as well. For a Wigley hull only Cartesian grids are used. However, the authors discuss the difficulties of resolving boundary layers on Cartesian grids, even at model scale Reynolds numbers and resort to using a body fitted solution from another code as boundary conditions for a far field solution using Cartesian grids. Other codes routinely use mixes of Cartesian grids in the far field and boundary fitted grids in the near field.

A new type of gridding approach is to use polyhedrons. Maki et al. (2007) demonstrate results with Fluent using polyhedral grids in the near field with hexahedral grids in the far field for a trimaran calculation. The polyhedral grids are constructed from typical unstructured tetrahedral cells so retain the ease of gridding associated with unstructured grids. Prism type layers of polyhedron are still used to resolve the boundary layer, but it is not necessary to do this for the free surface region. The polyhedron cells cut down on grid skewness and overall cell count leading to faster solution convergence. Very good comparisons of the resistance for the trimaran



were shown, but it was necessary to use the experimental values of sinkage and trim.

Overset, or chimera, grid technologies also remain popular to ease gridding difficulties. Noack (2007) provides an introduction to the overset grid methodology and how it is being used in marine hydrodynamics for complicated geometries, such as shafts and struts on a hull, relative motion between components and large amplitude motions. Separately, Noack (2005), describes the Structured, Unstructured, and Generalized overset Grid Assembler (SUGGAR) code, which provides a general overset grid assembly capability that can create domain connectivity information for various cell types and has been implemented in a number of RANS codes. Overset grids have been demonstrated in a number of computations including: the fully appended Athena by Bhushan et al. (2007) and the KRISO LNG Carrier by Kim et al. (2007). Overset grids are a convenient way to include the appendages in a computation. Regnstrom and Bathfield (2006) also applied an overlapping structured grid method to the computation of the flow around two ship hulls with appendages at both model and full scale. The ships are a frigate with sonar dome, bilge keels, propeller shafts, brackets, nozzles and rudder and a hopper-dredger with head-box, shafts, brackets and nozzle. As described by the authors the overlapping grid method made it easy to include or exclude appendages from a computation without having to regenerate the whole grid.

Carrica et al. (2006) used overset grids for ease of gridding appendages on the R/V Athena, but also showed how using dynamic overset grids could be used to allow ship movement to allow for sinkage and trim changes as part of a resistance prediction. This dynamic overset gridding was also used by Miller et al. (2006) and Stern et al. (2006a) for high speed ships discussed later.

Unstructured grids are still of great interest to the community as a way to ease the gridding

of complicated geometries. However, the unstructured grids also present their own problems for generating good resolution around the free surface for surface capturing methods. Often prism layers are needed near the hull to predict boundary layers accurately. As shown by Gorski et al. (2007) the boundary layer prediction can be directly dependent on the number of prism layers in the boundary. The difficulties with unstructured grids were further mentioned by Wood et al. (2007) who attempted to use unstructured grids with CFX for the DTMB 5415. Prism layers were used near the walls and around the free surface, but because poor results were obtained with the unstructured grids the authors resorted to structured grids for the data comparisons. Wilson et al. (2007b) also used prism layers around the free surface. They further discuss for DTMB 5415 how tetrahedral elements in the sonar dome wake region led to excessive diffusion of the sonar dome vortex and it was necessary to resort to a band of hexahedral elements around the sonar dome and in its wake region. Hino et al. (2006) demonstrates a number of predictions using a code developed for unstructured calculations. For bare hull calculations of the KVLCC2 and KCS structured grids are used. However, for more complex geometries, which include shafts and struts or a podded propulsor, unstructured grids are used. Prism layers appear to be used near the walls. However, for an azimuth propulsor calculation on a chemical tanker, Hino (2007) uses structured grids. Visonneau et al. (2006) also touch on the accuracy of hexahedron cells and using them in an unstructured framework can lead to fast grid generation over conventional block structured meshes. The weak point is the local loss of accuracy near the locally refined faces where misalignment and non-orthogonality are very high and reduce the local accuracy.

Another feature of unstructured grids is the potential for doing local grid adaptation as demonstrated by Leroyer et al. (2005) who implemented an adaptive mesh capability with their unstructured code to dynamically

maintain a prescribe density of grid points around the air water interface with their surface capturing method.

Resistance prediction accuracy is dependent on the particular grid chosen for resolving the geometry and flow field. Eca and Hoekstra (2005) performed double body calculations of the KVLCC2M tanker using a number of single block structured grids of the H-O and C-O type. They showed the predicted frictional resistance was not overly influenced by the grid topology or node distribution. However, the pressure resistance was very sensitive to the gridding, particularly around the bow. One issue with many of the calculations being performed and the uncertainty analysis is that the grids are not yet in the asymptotic range.

Turbulence Modeling. Although linear eddy viscosity based models are still the most often used turbulence models for ship flows there continues to be papers with higher order closure models, particularly for predicting flow details. The main problem with higher-order closure models has often been their numerical difficulties more so than their modeling deficiencies. Hanjalic (2005) notes that RANS models are witnessing a renaissance as various groups have worked to make the higher order models more robust for industrial applications so that they can better impact design.

Numerical Solution Methods. Efforts are still being pursued to make progress with the Smoothed Particle Hydrodynamics (SPH) method for ship flows. Oger et al. (2006) demonstrated some success in predicting wave fields for a three-dimensional ship hull with the SPH method, but no resistance predictions are described in the effort.

LES, Hybrid RANS/LES and DES Methods. These methods continue to be of interest as computer power increases. Hybrid RANS/LES methods are more routinely being done than in the past, often as part of a RANS computation, where more flow detail is shown with the hybrid method than with the RANS.

For a surface piercing foil and cylinder Kim and Cokljat (2007) used a volume-of-fluid technique with both LES and DES. In the near field the DES approach provides less free surface detail and unsteadiness than the full LES simulation, primarily due to the RANS turbulence model. The LES solution however, degrades quickly away from the geometry as the mesh becomes coarse, whereas the DES performs well away from the geometries and reproduces the Kelvin wave system. Xing et al. (2007) also computed the surface piercing foil with DES.

The Karman-like shedding from a transom has also been investigated (e.g. Bhushan et al. 2007), using DES and unsteady RANS. Significant differences in shedding frequency can be obtained based on which approach is used. In addition, differences in the shedding frequency between bare and appended hulls may be due to grid resolution.

LES simulations are still much slower than RANS and many feel LES techniques will likely not be a real design tool anytime soon. Conversely, Bensow et al. (2006) argue the cost of LES is becoming manageable with the use of massively parallel computers and subgrid wall models. They have compared the predictive capabilities of RANS, DES and LES by performing simulations of the flow around a 3D surface mounted hill in a channel and the flow past an axisymmetric hull. They state that both LES and DES are more accurate than RANS because RANS removes virtually all of the dynamics of the large, energy containing eddies, and no turbulence model can alleviate this. Whether LES becomes a design tool or not LES simulations can provide valuable insight into flow physics. However, as discussed by Hanjalic (2005), one must also be cautious of LES predictions, particularly on coarse grids for wall bounded flows as, the results can be wrong and worse than conventional RANS.



5.4 New Applications

Propulsor/Hull Interaction. There continues to be computations for propelled ships and a number have appeared in the literature. One example is that of Tahara et al. (2006) using two different RANS codes for the KCS in both towed and self-propelled conditions with an actuator disc model. The improved gridding capabilities available with overset grids have led to continued predictions of fully appended hulls, often with actuator disc models, to simulate the propeller. One example is the flow over the Athena predicted by Bhushan et al. (2007) who demonstrate the flow off of the shafts and struts. The KRISO LNG Carrier is predicted by Kim et al. (2007) for the fully appended and propelled configuration where thrust deduction, wake fraction, propeller and hull efficiency are compared with experimental data. The interaction of the propelled wake with the rudder is also examined, which compares well with experimental data demonstrating RANS codes can adequately predict propulsor-hull-rudder interactions.

Drag Reduction. A number of papers related to the prediction of the drag reducing properties of microbubbles and polymers appeared in the literature (e.g. 2nd International Symposium on Seawater Drag Reduction, ISSDR 2005). However, most of these papers were very fundamental concentrating on flat plate boundary layers and the modeling needed to represent the correct physics. One practical application is that of Choi et al. (2006, 2007) who demonstrated the potential for predicting the resistance of a hull with an air plenum using a boundary element code. The authors predicted the trends for a variety of air plenum and hull form parameters.

High Speed Vessels. High speed vessels received attention from a number of authors using both inviscid and viscous prediction methods. Ando, Yoshitake and Nakatake (2005) developed a combined Rankine source and panel method for the prediction of catamaran and trimaran hulls and showed the

impact of stagger on the wave making resistance of the hulls both numerically and experimentally. Miller et al. (2006) performed resistance, sinkage, and trim calculations over a large range of speeds for the R/V Athena Model 5365 and a high speed sealift trimaran concept. Full speed range resistance curves were obtained using a “numerical tow tank” concept by slowly accelerating the ship from $Fr = 0.0$ to 1.0. In addition, self-propulsion of the R/V Athena appended with skeg, stabilizers, shafts, struts, and rudders is simulated for two Froude numbers in the free to sink and trim mode. Preliminary calculations for the R/V Athena fitted with waterjets were also performed illustrating the above waterline jet discharge impacting the transom wake. A more comprehensive effort is documented in Stern et al. (2006a) who evaluated a suite of computer codes for hydrodynamic design including fast inviscid codes for the initial parametric studies and gross optimization, followed by unsteady RANS for detailed optimization and evaluation of ship performance. The paper describes the development, initial evaluation, and initial validation of this suite, applied to analysis of high-speed multihull transport ship design concepts. The capability of the design suite to meet the naval architect’s needs is demonstrated, at various stages of the design, and the codes are validated with available data. Maki et al. (2007) also showed that good predictions for a high speed trimaran could be obtained with thin-ship theory and the ITTC friction line. However, even better results were obtained by them with RANS when using the experimentally provided sinkage and trim. Another example of a trimaran calculation is that of Sato et al. (2007), which showed good comparison of resistance, sinkage and trim with a RANS code for different side hull positions.

5.5 Conclusions

Computational capabilities are making inroads in the design and evaluation processes

for many vehicles of interest including marine vehicles. Inviscid methods are still often used, but RANS codes, DES and LES are starting to play a larger role in the study of viscous flow fields generated by marine vehicles. It is inevitable that these methods will have an even larger role in the future as computer power increases and the application of such codes further matures. However, it will still take considerable effort to have the confidence in these methods that currently exists with the model tests as grid resolution and turbulence modelling drives the accuracy of the solution.

6. VALIDATION OF PREDICTION TECHNIQUES

6.1 Introduction

This section reviews recent activities in the field of verification and validation (V&V) considered to be of significance for the members of ITTC. Some papers thoroughly summarising general aspects of V&V have also appeared recently.

Oberkampf et al. (2004) and Stern et al. (2006c) have discussed all aspects of V&V. These papers additionally cover some of the issues related to achieving consensus on verification and validation. Stern et al. (2006c) have also broadened the discussion from just V&V to quantitative certification of CFD codes. Roy (2005), on the other hand, presents a review focusing on code and solution verification in computational physics with the emphasis on solution verification and error estimation methods based on Richardson extrapolation.

6.2 Workshops Related to V&V

1st and 2nd Workshop on Uncertainty in CFD. Two workshops concentrating on different aspects of verification, with validation purposely left out, have been organised within

the past few years by Luis Eca and Martin Hoekstra in Lisbon (Eca and Hoekstra, 2004; 2006d). The first workshop focused on solution verification with two simple two dimensional test cases and grids provided by the organisers: flow over a hill and flow over a backward facing step. In the second workshop the dual nature of verification, i.e. code and solution verification, was emphasised with a separate test case for code verification (see Section 6.5). For continuity with the first workshop the backward facing step case was also used in the second workshop as the test case focusing on solution verification. Unlike in the first workshop, participants were free to choose their grids giving an impression of the effect of grid layout. The entries in the workshops have covered a range of turbulence models, discretisation schemes and uncertainty estimation methods.

In the first workshop, despite some issues with oscillatory convergence, gratifyingly consistent results were obtained providing a favourable evaluation for the uncertainty estimation approaches. The goal of overlap of uncertainty estimates was essentially met with some exceptions. In the second workshop, the results were twofold. Very positive results were obtained for the code verification case, whereas for the back step problem the results were not as conclusive – apparently due to variation in the modelings used and problems in reaching the asymptotic range. Nevertheless, it was concluded, based on combining the results from both workshops for the back step problem, an encouraging consistence is shown. Even if there is some variation in the solutions due to modeling and numerics, the error obtained by several different methods appears realistic and generally consistent.

A third workshop has been announced to be held in 2008. The future workshop will cover all three steps of V&V, i.e. code verification, solution verification and validation.

CFD Workshop Tokyo 2005. The workshop (Hino, 2005) was fifth in a series of



workshops on CFD in ship hydrodynamics. It was reviewed already in the previous ITTC RC report, but some additional analysis of the results has been performed for this report. A specific test case (Test case 5, KVLCC2M without free surface) for the application of standard methodology for verification and validation of CFD methods was setup. Five geometrically similar O-O topology structured grids with grid points ranging from 158k to 9.6M were provided by the organisers. Verification and validation has been performed also for some of the other cases by some participants (case 1.1, KCS with free surface and fixed sinkage and trim; case 1.2, DTMB 5415 with free surface and fixed sinkage and trim; case 1.4, as case 5, but with own grids). For the integral quantities the validation uncertainty has been reported in 33 cases. Table 6.1 summarises the validation results for these indicating the corresponding test case, the number of validated cases over the total cases with reported validation uncertainties and the level of successful validation.

Table 6.1: Summary of the validation results from the Tokyo CFD Workshop.

Case	Validated/Tot	Validation level %D
1.1	2/5	2.2-2.4
1.2	1/3	9.8
1.4	5/9	3.3-7.9
5 (g2)	2/4	.92-3.3
5 (g3)	3/6	1.7-18
5 (g4)	1/3	4.5
5 (g5)	1/3	91

The workshop has also revealed some issues regarding verification and validation. The quality of the common grids has not been sufficient for converged solutions, and it has been stated that generation of common grids in studies like this is a nontrivial task due to the differing requirements of the codes. Furthermore, it has been demonstrated in several cases that using an uncertainty estimator based on a profile average for bounding the local error has often failed,

particularly for bow and stern waves as well as wake peaks, whereas local error estimators perform significantly better.

6.3 Examples of other Systematic V&V Studies

Werner (2006) has conducted a comprehensive study on different methods for verification and uncertainty analysis of CFD results. Three different methods, including the recommended procedure by ITTC, have been applied to an analytical boundary layer test case. Di Mascio et al. (2007) have also used the ITTC recommended procedure for the verification of a single-phase level set method and for the validation of numerical results obtained with the approach. Three two- and three-dimensional test cases have been used: flows around a submerged hydrofoil and Series 60 in non-breaking wave conditions and, as a practical application, a naval combatant in both non-breaking and breaking wave conditions. The validation has concentrated on force coefficients, but some order of accuracy studies have also been presented for the field variables as well as the wave height. For the uncertainty analysis with 'Le Commandant Riviere' Visonneau et al. (2006) have used the ITTC procedure for convergent cases and for divergent cases they have used the approach proposed by Eca and Hoekstra (in Eca and Hoekstra, 2004), based on the data range.

The revised version of the ITTC procedure has been used by Kim et al. (2006) for the verification and validation of the steady thrust, torque and radial velocity of the P5206 nozzle propulsor. Wilson et al. (2006) have applied the procedure to validate the unsteady numerical simulation of a roll decay test of the DTMB5512 surface combatant with bilge keels. Comprehensive verification and validation has been performed using the L2-norm of the difference of the roll motion time histories in order to evaluate iterative, grid and time step based uncertainties and to validate the simulation results against measurement data.

An example of the application of an alternative uncertainty estimation approach has been presented by Toxopeus (2005). He has evaluated uncertainty estimates for the simulated force and moment coefficients of KVLCC2M with several drift angles using the least squares version of the Grid Convergence Index (GCI) procedure proposed by Eca and Hoekstra (2002).

Finally, on a related topic, Stern et al (2006c) developed a quantitative certification procedure for assessment of probabilistic confidence intervals for CFD codes for specific benchmark applications and certification variables. Using the developed procedure they have presented an example of quantitative certification of RANS codes for ship hydrodynamics using the simulation results of different codes for the KVLCC2 from the Gothenburg 2000 CFD Workshop.

6.4 Iterative Convergence

Verification and validation studies presented in the literature concentrate mostly on grid convergence and, in the case of unsteady simulations, also on the convergence of the temporal discretisation. However, the importance of the numerical error from incomplete iterative convergence has also been considered in several papers. Often the iterative error has been shown to be negligible compared to the discretisation errors (e.g. Wilson et al., 2006; Di Mascio et al., 2007).

Eca and Hoekstra (2006c), on the other hand, have conducted an extensive systematic study on the iterative error. They present a procedure for evaluation of the iterative uncertainty based on a least squares fit to the iteration history of the norm of the variable change or the normalized residual. They have also studied the importance and influence of the iterative error on the discretisation error using three test cases: a two dimensional flow over a hill, a three dimensional flow over a finite plate and the flow around the KVLCC2M

at model scale. The results show that with insufficient iterative convergence the discretisation error depends on the iteration level. It is stated that, in order to have discretisation error independent of the iteration level, the iterative error should be two to three orders of magnitude below the discretisation error. This is in line with the statement by Roy (2005) that the iterative and round-off errors should be at least 100 times smaller than the discretisation error to ensure that they do not adversely impact the order of accuracy calculation.

6.5 Method of Manufactured Solutions (MMS)

The method of manufactured solutions has become an established tool for code verification. A number of papers can be found in the literature covering both the method itself as well as application examples for code verification. In his review paper on code and solution verification Roy (2005) spends a significant amount of space discussing MMS. Salari and Knupp (2000) have devoted a full report on code verification with MMS discussing the fundamentals of MMS and presenting some examples of code verification. The report includes an exhaustive example, in which MMS has been used to find intentional coding mistakes in a two dimensional compressible Navier-Stokes solver. Out of the twenty-one mistakes introduced in the code, MMS detected all of the coding mistakes, which prevented the governing equations from being solved correctly.

MMS has also been used in the 2nd Workshop on CFD Uncertainty Analysis (Eca and Hoekstra, 2006d) discussed in Section 6.2. A test case with manufactured solutions for a turbulent flow over a flat plate was introduced in order to help assess the reliability of uncertainty estimators vs. errors in the code implementation. A range of different turbulence models, discretisation schemes and uncertainty estimators were used by the



participants. The MMS results were very positive and consistent with 95% certainty for the error bars. Out of nearly a hundred cases 98% gave conservative estimates, i.e. the uncertainty bounded the error.

Eca and Hoekstra (2006b) have studied the influence of the discretisation of the turbulent quantities on the order of convergence of velocity and pressure using two manufactured solutions valid for 2D RANS equations supplemented either with the Spalart & Allmaras one-equation turbulence model or with a two-equation k - ω turbulence model. Three types of exercises have been performed: solution of the velocity and pressure with the manufactured eddy viscosity and vice versa as well as solution of the complete field.

The application of MMS for code verification is, however, not without some issues. For example, Eca and Hoekstra (2006a) discuss the difficulties in setting up manufactured solutions for the turbulence quantities in one and two equation eddy viscosity models. They state that the existence of damping and blending functions including non-linear equations and undefined derivatives is problematic for the application of the MMS.

6.6 Verification for Large Eddy Simulation (LES)

Verification methodologies for general CFD perform poorly with LES. One problem with LES in this regard is that both the numerical and the subgrid model depend on the grid resolution. In LES the grid resolution should be such that the stresses related to the numerical error are significantly smaller than the stresses from the subgrid model. On the other hand, the a posteriori formulations for estimation of numerical uncertainty for general CFD are too laborious to be used with LES. Because of these problems, some verification methodologies specifically for LES have been proposed recently.

Celik et al. (2005b) have proposed various indexes based on the Richardson extrapolation concept for assessment of the resolution quality (verification) of LES simulations. The proposed index measures the ratio of the resolved and total turbulent kinetic energy. The performance of the index is demonstrated with various cases, and comparisons with direct numerical simulations (DNS) and experiments show that the index is a good indicator of resolution quality for LES.

An alternative procedure has been proposed by Jordan (2005). He presents a quantitative local method for estimation of the uncertainty, which is performed before statistical averaging. The a priori estimate of the uncertainty is based on the area under the spectra of dimensionless turbulence quantities, where the unresolved part is modeled. With the proposed method, an estimate for the uncertainty is possible already with one LES-simulation, but a more accurate estimate is provided by using a second solution and a Richardson extrapolation based estimate. The method has been tested with several cases using measurement and DNS data.

A fundamental study on the numerical and modeling error of LES has been conducted by Brandt (2007). A case was studied in which second-order finite-difference schemes and simple subgrid scale (SGS) models are applied for a fully developed turbulent flow between parallel walls. The choice has been motivated by two reasons: these are often used in practical LES and some reports have been made on large numerical error related to low-order finite-difference-type schemes. An a priori study of the error components with focus on explicit filtering of the nonlinear convection term suggests that explicit filtering effectively reduces the numerical error and increases the effect of the SGS model. However, in the actual simulations, the explicit filtering increased the total simulation error. Based on a posteriori tests using grid independent LES, the numerical and modeling errors with standard Smagorinsky models are of the same order of magnitude and explicit filtering introduces a

third error component, which is larger than the other two. Of the applied approaches, the a posteriori tests explain the behavior of the actual simulations, whereas the numerical error predicted by the a priori tests is too large and the effect of SGS modeling and explicit filtering are not properly described.

6.7 Issues in V&V

Despite the established research there are still several issues related to verification and validation studies. Fundamental issues related to grid convergence have been discussed in several publications. The problem of reaching the range of asymptotic grid convergence has been studied thoroughly by Eca and Hoekstra (2006d). The same problem has also been discussed at the CFD Workshop in Tokyo (Hino, 2005). Similarly, Salas (2006) has considered issues and necessary conditions to properly establish grid convergence with focus on unequal refinement in different coordinate directions. Relatedly, Wilson et al. (2007a) discuss the coupling of the modeling and the numerical error, when studying the breaking bow wave of the DTMB 5415 surface combatant. The breaking bow wave is associated with a wide range of temporal and spatial scales with a trend of resolving finer scales with grid refinement. They state that, in terms of free surface details, it is presently not practical to obtain three solutions in the asymptotic range for this case.

Oscillatory convergence, for which Richardson extrapolation cannot be used, has been one of the main issues at the 1st Workshop on Uncertainty in CFD (Eca and Hoekstra, 2004) – especially for the convergence of the local values. Celik et al. (2005a) have discussed some possible remedies in this regard. They have exhibited the existence of oscillatory convergence by constructing schemes with a discretisation error satisfying oscillatory function, when applied to a simple convection-diffusion equation. By constructing model error equations and by

using these to ensemble a large number of cases with oscillatory convergence, the performance of four different extrapolation methods has been tested.

The simulations for bare-hull and appended configurations of the frigate 'Le Commandat Riviere' by Visonneau et al. (2006) demonstrate further issues directly related to grid convergence – namely the observed order of accuracy differing considerably from the theoretical order of accuracy and monotonic divergence, especially with unstructured grids. It has been suspected that the problems are related to difficulties in ensuring geometric similarity between different unstructured grids. Issues with complex geometries, e.g. prohibitively high grid resolution requirements, are also discussed in the paper as well as in Starke et al. (2006). On a related topic, Tahara et al. (2006) discuss issues with multiple grid studies using overlapping grids, where, in addition to the extra resources required for the multiple grid study, overlap on the finest grid has to be increased in order to provide sufficient overlap on the coarsest grid.

The severe grid dependency exhibited particularly by the pressure resistance has been discussed in several papers (e.g. Visonneau et al., 2006; Raven et al., 2006). Furthermore, Raven et al. (2006) give one example of an implementation issue, namely the implementation of the symmetry condition at the still water plane, which in the authors' method appeared to have a significant effect on the viscous pressure resistance and the associated grid dependency. Eca and Hoekstra (2006b), on the other hand, demonstrate using MMS that the order of accuracy of the discretisation of the turbulent quantities may influence the order of convergence of the other flow quantities. They also discuss some of the issues related to grid convergence and error estimation, when flux limiters are used.



6.8 Conclusions

Despite the existence of established procedures for verification and validation of CFD simulations, the number of studies including quantitative uncertainty analysis with systematic procedures has not increased significantly. Grid or parameter dependency studies are often only of a qualitative nature with an aim to demonstrate that the grid resolution used is sufficient (in some sense). Nevertheless, the studies, which include quantitative uncertainty estimation, are increasingly more rigorous for a wider range of applications, such as unsteady and unstructured cases.

For example, several authors at the 10th Numerical Towing Tank Symposium (Bertram, 2007) have considered issues with discretisation accuracy. Mostly this was in the form of qualitative studies indicating the level of e.g. grid dependency without quantitative uncertainty estimation. However, there were also examples of quantitative uncertainty estimation using the procedure by Eca and Hoekstra (2006c) for an open water simulation of a propeller and code verification exercises for unstructured flow solvers using MMS – including the verification of a time accurate free surface tracking code.

As shown by the results of the 1st and 2nd Workshop on CFD Uncertainty Analysis, the established uncertainty estimation procedures give encouragingly reliable estimates of the numerical uncertainty. However, there are still considerable problems in applying systematic procedures for a variety of simulation cases, especially as the complexity of the simulated cases increases and the simulation methods become more sophisticated.

Therefore, the ITTC continues to encourage the use of uncertainty estimates for CFD studies and should continue to monitor the development of procedures for estimation of the numerical uncertainty with emphasis on practical application issues and the evolving

complexities. The ITTC should maintain its procedure 7.5-03-01-01 “Uncertainty Analysis in CFD, Uncertainty Assessment Methodology and Procedures” with the revisions from the 25th ITTC RC.

7. FACILITY BIAS WORLD WIDE CAMPAIGN

The 24th ITTC Resistance Committee invited all the ITTC members to participate in a worldwide series of comparative tests for identifying facility biases under the framework of ITTC procedures for uncertainty analysis. For these tests two geosims of the DTMB 5415 Combatant with 5.720 and 3.048 meters length, respectively, have been used.

The Committee created and distributed a technical procedure for identifying facility biases, compiling model and test procedure information, including data submission guidance to preserve the confidentiality of the data.

Facility biases have been analysed for the following most typical towing tank tests:

- Resistance
- Sinkage and trim
- Wave profile and wave elevations

7.1 Participants

As result of the 24th ITTC, the number of Institutions participating in this worldwide series for identifying facility biases was increased from twenty to thirty five and the number of countries was increased from fifteen to nineteen, with eighteen Institutions testing each model. A new schedule was arranged in order to finish the tests on time for the 25th ITTC. Nevertheless, there were many delays and many Institutions did not test the model on time. The provisional schedule, indicating the month of reception of the model, is summarized in the following tables.

Table 7.1 Schedule for the 5.720m length model.

Institution	Country	Month
CEHIPAR	Spain	Jun 2004
INSEAN	Italy	Sep 2004
Helsinki University of Technology	Finland	Nov 2004
Krylov Shipbuilding Research Institute	Russia	Feb 2005
ICEPRONAV S.A.	Romania	Sep 2005
Vienna Model Bassin	Austria	Dec 2005
Huazhong University of Science and Technology	China	-----
CSSRC	China	Sep 2007
Samsung Ship Model Basin	Korea	Dec 2007
MOERI	Korea	Feb 2008
Pusan National University	Korea	Apr 2008
Akishima Laboratories	Japan	Jul 2008
NMRI	Japan	Aug 2008
IHI Corporation	Japan	Sep 2008
Naval Surface Warfare Center	USA	Dec 2008
Institute for Ocean Technology	Canada	Feb 2009
QinetiQ	UK	May 2009
Bassin d'Essais des Carenes	France	Aug 2009
CEHIPAR	Spain	Oct 2009

Table 7.2 Schedule for the 3.048 m length model.

Institution	Country	Month
CEHINAV	Spain	Feb 2005
LSMH/NTUA	Greece	Apr 2005
Inha University	Korea	Dec 2005
Seoul National University	Korea	Jan 2006
Pusan National University	Korea	Feb 2006
Ulsan University	Korea	Mar 2006
Harbin Engineering University	China	-----
University Teknologi Malaysia	Malaysia	Sep 2006
Australian Maritime College	Australia	Nov 2006
Canal de Experiencias de Arquitectura Naval	Argentina	Feb 2007
University of Iowa – IIHR	USA	Jul 2007
Stevens Institute of Technology	USA	Jan 2008
University of Glasgow and Strathclyde	UK	Mar 2008
University of Liège – ANAST	Belgium	Jul 2008
Ecole Centrale de Nantes	France	Oct 2008
Istanbul Technical University	Turkey	Feb 2009
INSEAN	Italy	May 2009
CEHIPAR	Spain	Aug 2009

Specific causes of the accumulated delay were:

- the 5.720 meters length model was confiscated due to problems in providing all the required documents while exporting it from Austria to China. Eventually it was brought back to China and tested at CSSRC, and could thus continue its circulation. A delay of 17 months was accumulated for this model;
- Ulsan University, failing to quarantine as required by China's customs, sent the 3.048m model to Malaysia, skipping Harbin Engineering University;

Other, general, causes were:

- the accumulated delays, the internal planning and the amount of work of the Institutions increased the testing periods;
- the required time to move the models between Institutions was higher than predicted.

7.2 Testing Procedure and Data Submission

Each institution has tested the model in 4 different sessions in order to change the test conditions and obtain better uncertainty analysis results. All the Institutions have used their standard techniques to test the model and have corrected their results taking into account the blockage effects, using their standard procedures.

Ten runs have been done each testing day with the following speeds:

Table 7.3 Froude numbers of the runs.

<i>Fr</i>	Session			
	1	2	3	4
Speed 1	0.28	0.28	0.28	0.28
Speed 2	0.10	0.10	0.10	0.10
Speed 3	0.28	0.28	0.28	0.28
Speed 4	0.41	0.41	0.41	0.41
Speed 5	0.10	0.10	0.10	0.10
Speed 6	0.28	0.28	0.28	0.28
Speed 7	0.41	0.41	0.41	0.41
Speed 8	0.10	0.10	0.10	0.10
Speed 9	0.28	0.28	0.28	0.28
Speed 10	0.41	0.41	0.41	0.41



The values corresponding to the first run of each session are not used in the analysis.

The following results of the tests have been submitted to the Resistance Committee using ASCCII neutral files:

Resistance. A data file has been sent for each session and speed, containing the following data, where biases and uncertainties were obtained using the ITTC recommended procedure 7.5-02-02-03:

- Session number
- Speed number
- Froude number, Fr
- Water temperature in centigrade degrees, t_w°
- Bias for the resistance coefficient C_T , B_{CT}
- Uncertainty for the resistance coefficient at 15 °C, $U_{CT}^{15 \text{ deg } C}$
- For each tested point:
 - Time in seconds, t
 - Velocity of the model in meters per second, V
 - Resistance measured in Newton, R_T

Sinkage and Trim. A data file has been sent for each session and speed, containing the following data, where biases and uncertainties were obtained using the ITTC recommended procedure 7.5-02-02-05:

- Session number
- Speed number
- Froude number, Fr
- Water temperature in centigrade degrees, t_w°
- Bow sensor position from section 0 in meters, x_F
- Stern sensor position from section 0 in meters, x_A
- Bias for sinkage, B_σ
- Bias for trim, B_τ
- Uncertainty for sinkage, U_σ
- Uncertainty for trim, U_τ
- For each tested point:
 - Time in seconds, t
 - Bow sinkage in meters, Z_{VF}

- Stern sinkage in meters, Z_{VA}

Wave Profile and Wave Elevations. Wave profile on the hull surface and a vertical longitudinal wave cut in a plane separated $0.172 \cdot L$ from the centre plane have been obtained for all the testing cases. A data file has been sent for each session, wave profile and wave cut, containing the following data, where biases and uncertainties were obtained using the ITTC recommended procedure 7.5-02-02-06:

- Session number
- Speed number
- Froude number, Fr
- Water temperature in centigrade degrees, t_w°
- Position of the sensor measured from centre line in meters, y
- Wave profile bias, B_ζ
- Product of wave profile bias and sensitivity coefficient in %L, $B_\zeta \theta_\zeta$
- Bias of the point position, B_x
- For each tested point:
 - x position along hull from section 0 (positive to bow) in meters, x
 - Wave profile height measured for each point of the hull, from calm water level (positive up) in meters, z

7.3 Analysis Method

The analysis method is based in $M \times N$ -order level testing, where N repetitions of the same experiment are done in each of the M different facilities participating in the experience. As it was stated by Stern et al. (2005) the medium value of a variable X , taking into account all the measurements done by all the facilities is

$$\bar{X} = \frac{1}{M \times N} \sum_{i=1}^M \sum_{j=1}^N X_i^j \quad (7.1)$$

Where X_i^j is the value obtained for the variable X in the text number j done in the facility i .

The uncertainty in \bar{X} is

$$U_{\bar{X}} = \sqrt{B_{\bar{X}}^2 + P_{\bar{X}}^2} \quad (7.2)$$

Where the bias and precision limits of the mean value of X are respectively $B_{\bar{X}}$ and $P_{\bar{X}}$.

The expression of the bias limit of the mean value of X is

$$B_{\bar{X}} = \frac{1}{M} \sqrt{\sum_{i=1}^M B_{\bar{X}_i}^2} \quad (7.3)$$

Where $B_{\bar{X}_i}$ is the bias limit of the mean value of X in the facility number i .

If the number of facilities involved in the tests is great enough the bias limit is almost zero because in equation (7.3) $B_{\bar{X}} \rightarrow 0$ when $M \rightarrow \infty$, and the mean value of the variable X can be considered as the true value of the measured variable for the uncertainty analysis.

The expression of the precision limit of the mean value of X is

$$P_{\bar{X}} = \frac{2}{\sqrt{M}} \sqrt{\frac{\sum_{i=1}^M (\bar{X}_i - \bar{X})^2}{M-1}} = \frac{2}{\sqrt{M}} \sqrt{\frac{\sum_{i=1}^M D_i^2}{M-1}} \quad (7.4)$$

Where \bar{X}_i is the mean value of X obtained from all the tests done in the facility i .

The uncertainty of the variable D_i , obtained for each facility as the difference between mean value of X using only their results and the mean value of X using the results from all the facilities, can be obtained from the following expression

$$U_{D_i} = \sqrt{U_{\bar{X}_i}^2 + U_{\bar{X}}^2} \quad (7.5)$$

Where $U_{\bar{X}}$ is obtained using equation (7.2) and $U_{\bar{X}_i}$ is the uncertainty value submitted by the facility i , obtained through ITTC procedures.

It is possible to calculate the uncertainty of the facility bias for the variable X in the facility i , U_{FB_i} by means of the following expressions

$$\begin{aligned} |D_i| \leq U_{D_i} &\Rightarrow U_{FB_i} = U_{D_i} \\ |D_i| > U_{D_i} &\Rightarrow U_{FB_i} = \sqrt{D_i^2 - U_{D_i}^2} \end{aligned} \quad (7.6)$$

This analysis process has been done for all the variables obtained for the tests.

7.4 Analysis Program and Available Data

Due to the number of calculations and the great amount of data used in the previous analysis method, a computer program has been done to facilitate the analysis of the data.

The delays in the schedule, commented on previously, have reduced the number of facilities analyzed for this Conference. Only 9 data CDs were submitted on time, 4 for the large model and 5 for the small one. One of the data sets for the large model was in a wrong format and was impossible to analyze. Some of the submitted CDs contained uncompleted or not well formatted data that has been re-structured, when possible, to be included in the analysis. In some cases only medium values are included in the submitted files.

The data for each model in the analysis program has been arranged in folders that have been numbered. The number of the folders does not correspond with the reception order or the test schedule, but with the amount of useful data received. This procedure guaranteed the confidentiality of the submitted data.

All data and the results of the analysis are available for all the ITTC members, so each Institution can identify its own data, and consequently its folder number, comparing the submitted data with the data available in each folder. The main results are summarized in the following sections.



7.5 Resistance Results

The following data is presented:

- The total resistance coefficients for each facility $(C_T)_i$ compared with their mean value $\overline{C_T}$.
- The uncertainties of the resistance coefficients for each facility $(U(C_T))_i$ compared with their mean value $\overline{U(C_T)}$.
- The uncertainties of the facility bias for each facility U_{FB_i} .

5.720 meters length model.

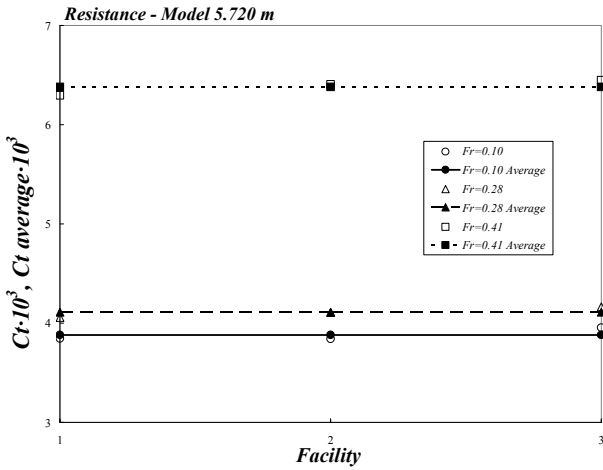


Figure 7.1 $(C_T)_i$ and $\overline{C_T}$

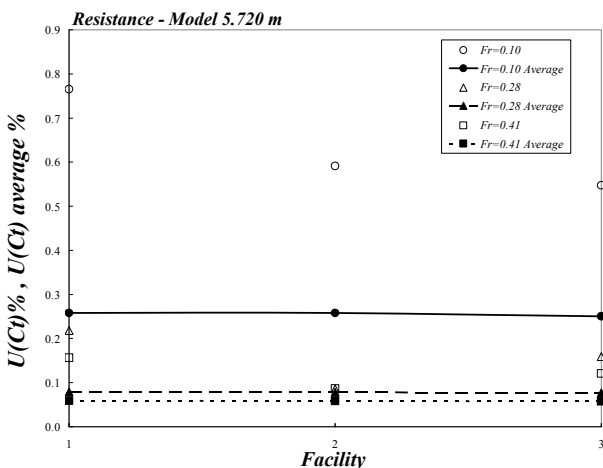


Figure 7.2 $(U(C_T))_i$ and $\overline{U(C_T)}$

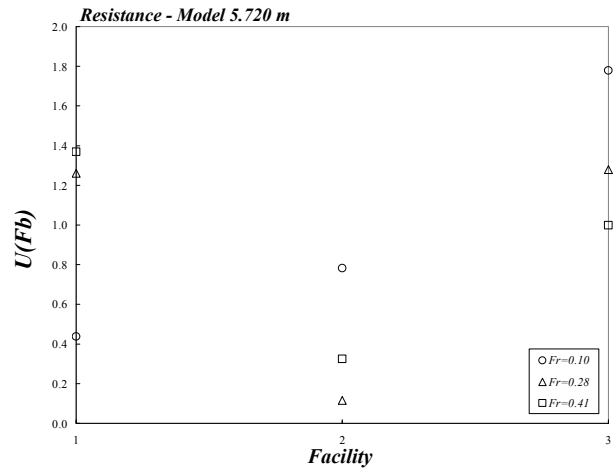


Figure 7.3 U_{FB_i}

3.048 meters length model.

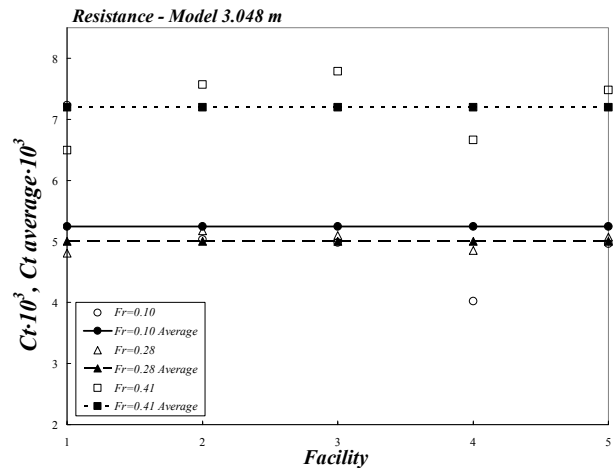


Figure 7.4 $(C_T)_i$ and $\overline{C_T}$

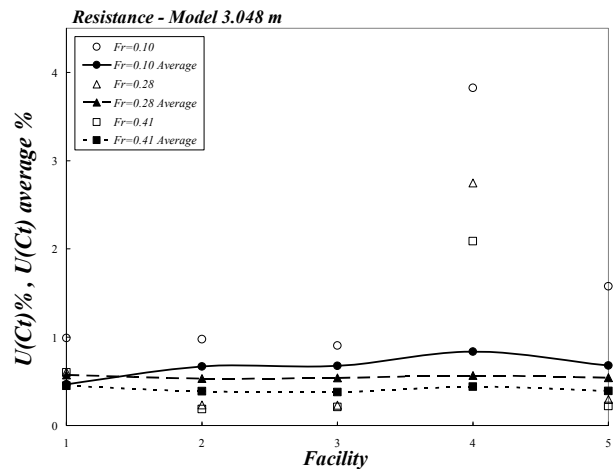


Figure 7.5 $(U(C_T))_i$ and $\overline{U(C_T)}$

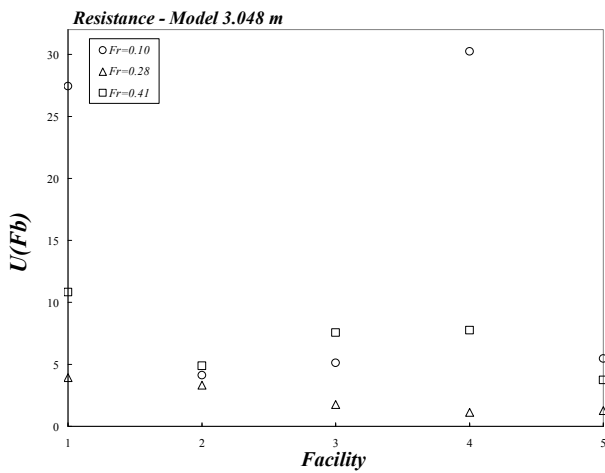


Figure 7.6 U_{FB_i}

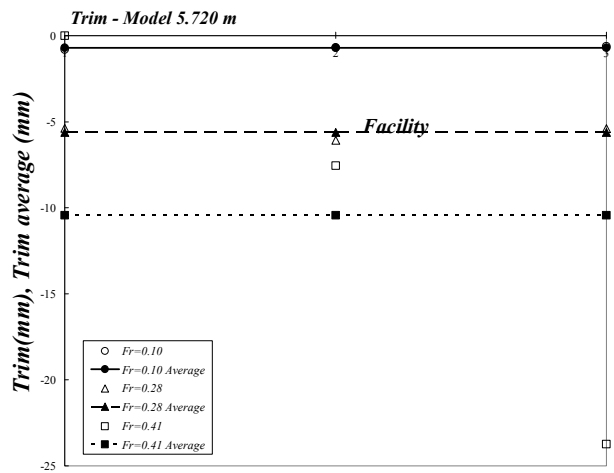


Figure 7.8 $(\tau)_i$ and $\bar{\tau}$

7.6 Sinkage and Trim

The following data is presented:

- The sinkages for each facility $(z_s)_i$ compared with the mean value for all the facilities, \bar{z}_s .
- The trims for each facility $(\tau)_i$ compared with the mean value for all the facilities, $\bar{\tau}$.
- The uncertainties of the facility bias for the sinkage for each facility, U_{FB_i} .
- The uncertainties of the facility bias for the trim for each facility, U_{FB_i} .

5.720 meters length model.

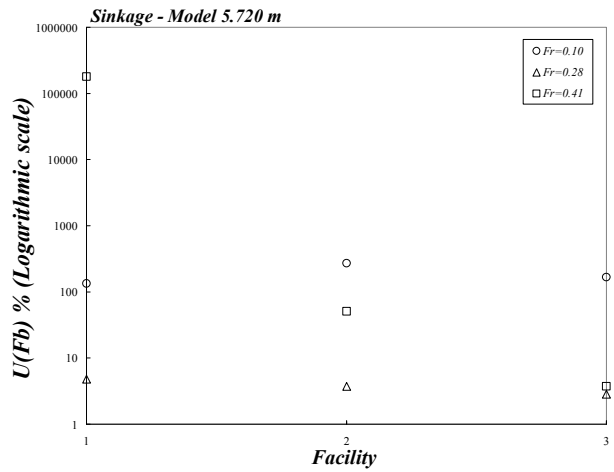


Figure 7.9 Sinkage U_{FB_i}

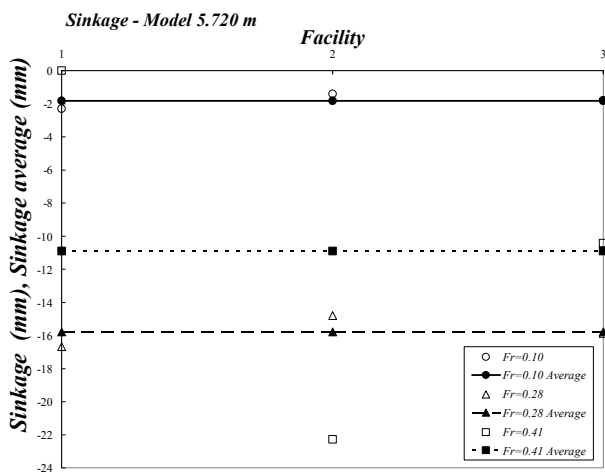


Figure 7.7 $(z_s)_i$ and \bar{z}_s

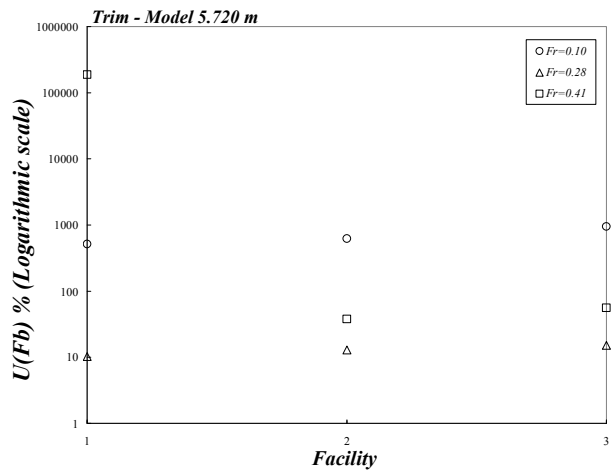


Figure 7.10 Trim U_{FB_i}



3.048 meters length model.

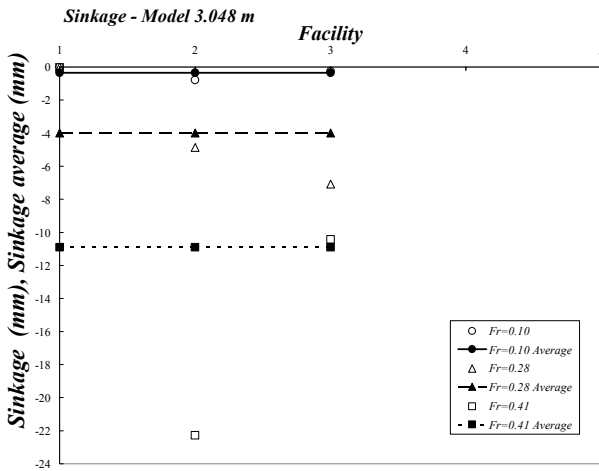


Figure 7.11 $(z_s)_i$ and \bar{z}_s

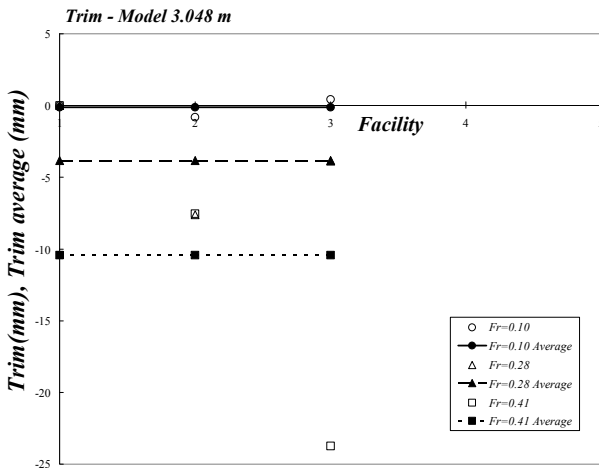


Figure 7.12 $(\tau)_i$ and $\bar{\tau}$

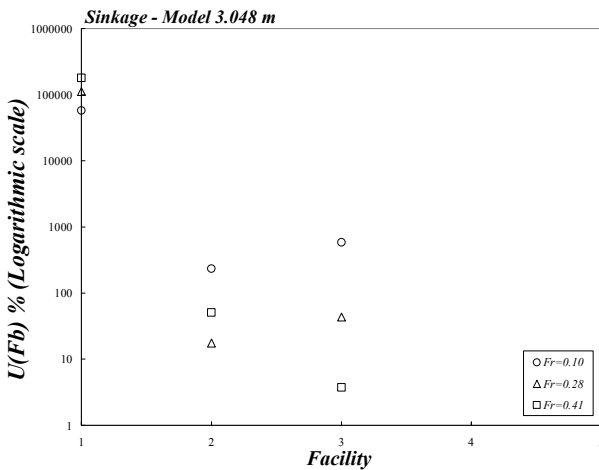


Figure 7.13 Sinkage U_{FB_i}

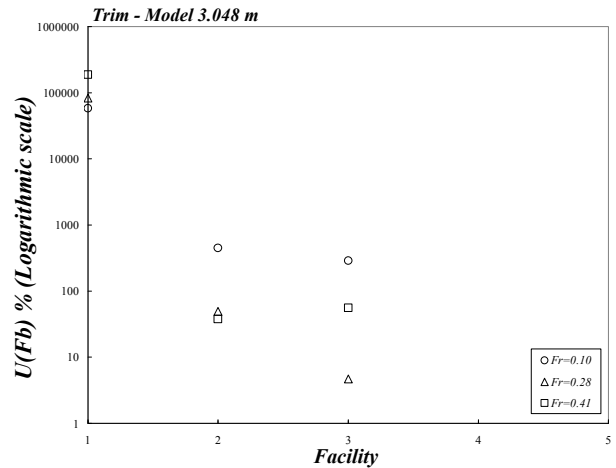


Figure 7.14 Trim U_{FB_i}

7.7 Wave Profile and Wave Elevation

Wave profiles and wave elevation uncertainties can be analyzed cutting the waves by a number of equally spaced sections. The following data was analyzed for each facility:

- Wave elevations for each facility $(\zeta)_i$ compared with the mean value for all the facilities, $\bar{\zeta}$.
- The uncertainties of the wave elevations for each facility $U((\zeta)_i)$ compared with the mean value for all the facilities, $\overline{U(\zeta)}$.
- The uncertainties of the facility bias for each facility, U_{FB_i} .

The number of wave profile and wave elevation files submitted is too short to be analyzed. Nevertheless the uncertainties of the facility biases for each facility in 20 sections along the hull U_{FB_i} are presented as an example.

Wave profiles and wave elevation analysis have presented some special problems due to the phase of the waves and the available data.

5.720 meters length model.

Only two facilities have sent wave profile data for this model. In both cases data was obtained only for one session and the data analyzed for the different sessions is a copy of

that. For this reason the quality of the analysis is not very good.

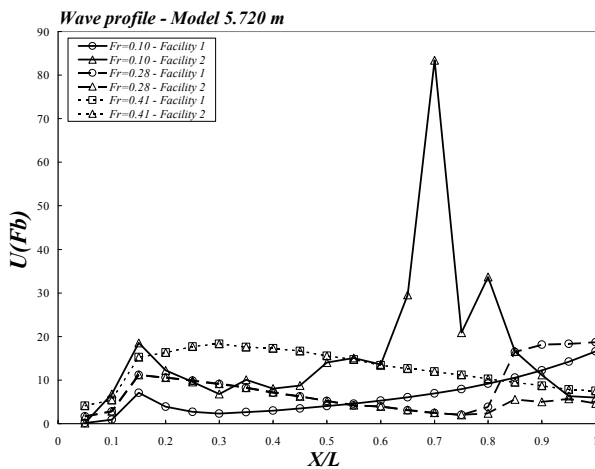


Figure 7.15 Wave profile U_{FB} example

Wave elevations in the cutting plane were not analyzed for $Fr = 0.1$ for this model, because the facility numbered as 1 did not submit data for this velocity.

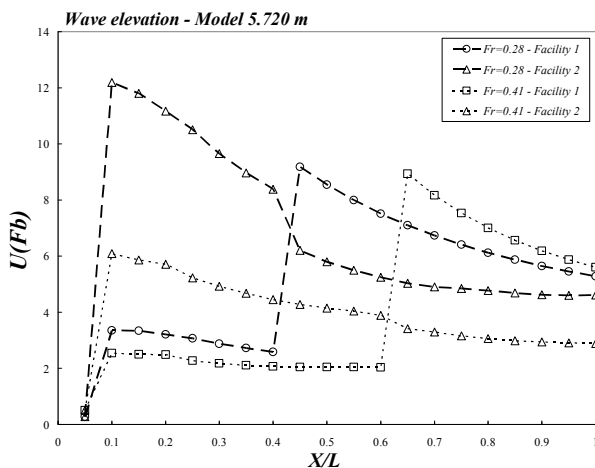


Figure 7.16 Wave elevation U_{FB} example

3.048 meters length model.

There is no wave profile data available for this model so only wave elevations in the cutting plane were analyzed for the two facilities that have sent data.

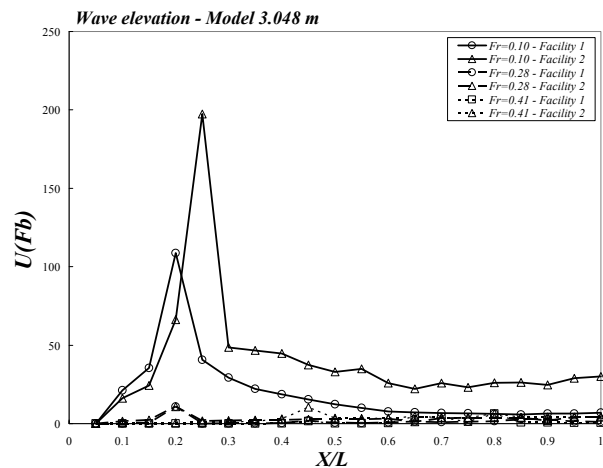


Figure 7.17 Wave elevation U_{FB} example

7.8 Conclusions

The following conclusions are obtained:

- Less than half of the facilities that have tested the model have sent the data on time to be analyzed. The Committee encourages all the participants to send their data as soon as possible.
- The submitted data was not always in the required format.
- All the facilities that have submitted data have calculated biases and uncertainties with the ITTC recommended procedures 7.5-02-02-03, 7.5-02-02-05 and 7.5-02-02-06 and their referenced worksheets.
- There are some resistance files presenting significant oscillations, even greater than the measured magnitude.
- Facility bias uncertainties are normally larger for the smaller Froude numbers.
- Sinkage and trim results are not available for all the facilities.
- The uncertainties obtained for the trim are very large in some cases.
- Only two facilities have sent wave profile data and in both cases data was incomplete. For this reason wave profile data could not be properly analyzed.
- Only four facilities, two for each model, have sent wave elevation data. For this reason wave elevations could not be properly analyzed.
- Wave elevation and wave profile analysis



have presented some special problems due to the phase of the waves.

- The amount of data used for the analysis was not enough to obtain valid conclusions about facility biases, but the analysis procedure has been developed to analyze the entire data set when available.

8. DESIGN METHODS AND OPTIMIZATION

Together with developments in CFD and computer power, the recent years have seen some progress in Simulation Based Design (SBD) for ships too. However, arguably, the initial excitement that accompanied the emergence of these techniques has diminished somewhat over the years, due to the fact that these methods are not as generally accepted or widely used in practical ship design as the optimization community initially hoped.

The explanation is not straightforward. It is certainly true that there are fundamental analytical and computational obstacles that must be overcome before SBD can make a widespread impact on the practice of ship design. Furthermore, robust and automated grid generation and manipulation has proved to be a serious challenge, as well as the need to account for complex, real-industrial geometrical and functional constraints, and the difficulty of generating the objective functions and their derivatives automatically and robustly when these functions are computed by solving Partial Differential Equations (PDE).

The potential benefits and pay-offs of the impact of SBD on the ship design process are so great, however, that despite the damping effects of reality on the immediate expectations, research on SBD has continued, yielding promising results and revealing specific new challenges and directions of research, which are briefly summarized in this chapter.

8.1 Methods and Problems

Variable Fidelity and Metamodels. For practical ship design problems, the major components of the cost of the design optimization are the analysis and the sensitivity computations. Savings in the computational cost can be achieved by making use of *variable fidelity* techniques (of three possible types, i.e. grid, physics, accuracy). The idea is to maximize the use of low fidelity, cheaper models in iterative procedures with occasional, but systematic, recourse to higher fidelity, more expensive models for monitoring the progress of the algorithm. Heuristic (i.e. trial and error) approaches have been largely used in the past, but substantial advances are due to the integrated use of variable fidelity ideas together with *trust-region* methods: the combined method is globally convergent to the solution of the original, high-fidelity problem (Alexandrov and Lewis, 2002). Additional savings in computational effort can be achieved by making use of *metamodels* (polynomial, spline, neural networks, kernel regression, etc.: for example see Jin et al., 2001), cheap and fast approximations of the objective function. Despite the obvious limitations imposed by sparse high fidelity data in high dimensions and the locality of low order polynomial approximations, metamodel approximations for SBD have become an important tool, capable of dealing with noisy functions and high computational cost. Goel et al., (2007) explore the possibility of using a weighted average surrogate model instead of individual surrogate models. Besnard et al., (2007) presented a Neural Network-based Response Surface Method for applications in ship design. The cost of the optimization is shifted to the generation of the data sets used for training the network. In Gano et al. (2004) a kriging based scaling function is introduced to better approximate the high fidelity response on a more global level and an adaptive hybrid method is also presented. A similar approach is suggested by Huang et al. (2006): a sequence of metamodels (kriging based) provides a global model of the objective function.

Examples of applications in ship design optimization are given in Peri and Campana (2005) and Campana et al. (2006).

Grid Regeneration and Deformation. A recent article by Samareh (2005) describes the major components required for using grid-based high-fidelity models in SBD: shape parameterization, automation of model abstraction, automation of grid generation, calculation of analytical sensitivity, and robust grid deformation. Among the available approaches, the use of the Free Form Deformation technique (Sederberg and Parry, 1986) is spreading at a fast pace (see for example Mason and Thomas, 2007). Direct use of B-spline surface fitting is also frequently used (Chen et al. 2006, Pérez et al. 2007). Another effective modeling methodology is the transfinite interpolation of an irregular network of curves (also referred as *H-rep* in recent literature, Veelo, 2004). The use of ship global parameters (such as length, beam, draft) is still widely used and seems more appropriate for defining design problems in the initial stage of the design process.

Derivative Based and Derivative Free Methods. The drawback in using accurate, high - fidelity models in SBD is that the function evaluations are expensive and computing accurate sensitivities for derivative-based optimization methods in such problems presents a challenge. The article by Martins et al. (2005) describes a coupled-adjoint method for computing derivatives in an aero-structural aircraft design framework, where high-fidelity models are used for both aerodynamics and structures. Ragab (2004) implements a continuous adjoint formulation on a panel solver. Martinelli and Jameson (2007) extended their adjoint based method to an incompressible flow with free surface using an Euler multigrid solver.

When the problem or the adopted solvers make it difficult to apply methods that require derivative information, *direct search* can be used. A complete and detailed review about

direct search methods capable of minimizing a function without recourse to its derivatives is given in Kolda et al. (2003). While the use of Genetic Algorithms is widespread, both in the binary and real-coded versions (see for example Tahara et al. 2007), other evolutionary techniques have been recently introduced, such as the Particle Swarm Optimization (PSO) method. For a recent review of PSO applications see the proceedings IEEE-SIS (2006) and Poli et al., (2007).

Uncertainty in Design Optimization. The growing need for safety and reliability at an acceptable cost necessitates the development of methods that yield robust designs, i.e., designs that are insensitive to variations in system inputs and other types of uncertainty. The article by Mattson and Messac (2005) addresses explicitly the multiobjective nature of MDO problems, decision making under uncertainty, and visualization techniques that assist in multiobjective decision making. Gumbert et al. (2005) present a simultaneous analysis and design strategy for MDO that accounts for the effects of propagation of geometric uncertainty on the formulation and compares the results to deterministic design. For a review on robust design methods see also Trosset et al. (2003). A recent application to ship design is presented in Neu et al. (2007).

8.2 Applications

It should be noted that SBD is not and, arguably, will never be push-button design. Rather, it is a tool that should provide the designer with rapidly generated alternatives while expanding the dimensionality of the design and function spaces, thus assisting the designer in exploring the design space more quickly, efficiently, and creatively.

Multihull optimization using SBD approaches has been presented in a number of recent papers. Doctors and Scrace (2003) optimized the configuration of a trimaran using a potential flow model.



Multiobjective problems have been solved by Zalek et al. (2006) (resistance and seakeeping) while Parsons et al. (2004) adopt a preference function approach that allow different multicriteria formulations to be computed with a conventional scalar method. Parsons et al. (2006) present an application to the design of stern flaps.

8.3 Conclusions

Ship design still implies great reliance on the *art* of engineering, the experience of the designer, and heuristic procedures. Nevertheless, the growing complexity of modern designs makes the use of heuristic methods alone increasingly challenging.

Radically new designs present a difficult problem because designers cannot rely on historical databases. Moreover, some areas of design experience a loss of immensely valuable design knowledge with the retirement of designers. There is also a realization that meeting a minimal set of requirements may not suffice to ensure success of new designs.

One should, instead, look for optimal designs, with increased reliance on rigorous computational methods. These causes motivate SBD, together with the development of better numerical models of the governing disciplines, faster optimization algorithms, and the ever increasing computational capacity.

9. FAR FIELD WAVES AND WASH

9.1 Introduction

Vessel wake wash (also commonly referred to as wash or wave wake) has been a prime topic for study over the past two decades, though it no longer attracts quite the same attention since industry has gained a general understanding of the primary issues. Reflecting this interest, the Resistance Committee has

been tasked to review wake wash prediction techniques over the past two ITTC terms. Given that much of the background to this topic has previously been covered, this latest review deals mostly with developments and studies published since 2005.

There are many references that provide background information, including a book authored by Lyakhovitsky (2007) which discusses in detail many hydrodynamic aspects of ship operation in shallow water, including a chapter on the environmental impacts as a result of ship generated waves. Murphy et al. (2006) conducted a literature review on research and current practice related to vessel wake wash to provide an overview of the findings, methodologies and mitigation strategies. The authors discuss many possible impacts that can be attributed to vessel wake wash, including: hydromorphological (erosion), ecological (aquatic plants, fish, macroinvertebrates, noise, water quality), and cultural heritage impacts.

Another recent general discussion paper is provided by Phillips and Hook (2006), who also provide an outline of Risk Assessment Passage Plans (RAPPs) which are required in the United Kingdom for all high-speed craft or any vessel that can potentially exceed $Fr_h > 0.85$. The authors also suggest that hazards can be split into 3 groups: close to sailing line, at a distance, at the shore. Hofmann et al. (2008) discuss the relative importance of both wind and ship waves on the shore of a large lake.

9.2 Prediction of Wake Wash Based on Experimental Measurement

The 2005 RC report described some of the challenges associated with the prediction of wake wash based on model test data, particularly in regard to limitations in facility width when measurements in the medium to far field are of more interest. It is likely that this has contributed to the increasing number of studies in recent years that have included the

conduct of site-specific full scale experiments, for example: Parnell et al. (2007), Soomere (2005), Velegrakis et al. (2006), Kumar et al. (2007), Varyani (2006), Balzerek and Koslowski (2007), Macfarlane and Cox (2004). As with any experiments conducted within uncontrolled environments there can be many factors that adversely affect the quality (and quantity) of experimental data, although some useful guidelines to minimise problems have been provided in some of the aforementioned references and in PIANC (2003).

Macfarlane (2006, 2008) has investigated the correlation between model and full scale wake wash data with generally good agreement. Unfortunately, there is still a lack of good quality, well detailed full scale data in the public domain that is suitable for the validation of CFD predictions.

Chalkias and Grigoropoulos (2007) carried out a series of experiments using large scale manned models to eliminate problems due to tank wall effects and reduced scale effects. These experiments were conducted in a sheltered waterway, where careful site selection can provide desired water depths. A real time kinematics (RTK) system was used to monitor the model track and speed with respect to the wave recording location. The authors also measured dynamic trim, heel and sinkage.

Full scale onsite experimental data has also recently been utilised to investigate the effects on riverbank erosion and to assist in the development of regulatory criteria, Macfarlane and Cox (2004, 2007), Macfarlane et al. (2008).

Robbins et al. (2007) conducted model scale experiments to show that the wave height decay coefficient of vessel generated waves varies with Froude depth number.

9.3 CFD Prediction

Linear Theory. Chalkias and Grigoropoulos (2005) investigate two methods of

applying a potential flow panel method to predict the near-field waves from four high-speed monohulls operating in deep water. The first method treats the steady flow as a special case of time-harmonic flow in the frequency domain. The second method is a sister method solving the time-domain flow. The solution algorithms are based on a 3-D Rankine Panel Method (RPM) where the two physical variables (i.e. the velocity potential and the free surface elevation) are represented with a higher order B-spline basis function. It is claimed that the methods are numerically stable resulting in no numerical damping and small numerical dispersion, so that there is no significant error in the free surface deformation. It is also claimed that the algorithms can handle transom sterns by applying a set of smooth detachment conditions of the flow at the transom and introducing a strip of 'wake' panels trailing the transom. The same authors also compare large scale experimental data with numerical predictions using the abovementioned linear code and nonlinear potential flow codes (SHIPFLOW), here the nonlinear code appears to produce the more favourable comparison, Chalkias and Grigoropoulos (2007).

Lazauskas (2007) contends that simple linear methods, such as Michell's thin-ship wave resistance theory can be extended and generalized to provide fast, accurate estimates of wave resistance and wave patterns, particularly for thin ships.

Nonlinear Theory. Soomere (2007) summarises the non-linear parts of a ship's wake waves, where the central topic is the generation of solitons by ship motion both in channels and in unbounded sea areas. There are 267 references cited in this review article. The optional non-linear components of ship wake such as the very narrow V-like wake components, packets of monochromatic waves, ship-generated depression areas, and supercritical bores are also discussed. A variety of different non-linear equations that have been used to study the generation of solitons are discussed, including: the Boussinesq equation,



the nonlinear (cubic) Schrodinger equation and its various generalizations, the Korteweg-de Vries (KdV), and the Kadomtsev-Petviashvili (KP) equations. Soomere (2006) provides further discussion on non-linear equations that have been used to study the generation of solitons, with particular emphasis on the KP equations

Soding (2006) suggests the use of nonlinear Rankine source methods to determine near-field waves followed by a constant-depth method (with the vessel either travelling in a straight course or a curved path) to model the far-field waves. The waves within an analysis rectangle behind the ship are used to extrapolate the wave field up to an arbitrarily large distance. The wave field is approximated as a superposition of regular, linear deep-water or shallow-water (Airy) waves. If the far-field waves are in a region possessing variable depth (with small variations in slope), then it is suggested that the number of dimensions can be reduced by one by substituting the time variable with a frequency variable and approximating the dependence of flow variables on the vertical coordinate by that of a regular wave of low steepness on a horizontal bottom. This is achieved for each wave frequency separately.

Soding also suggests that the predictions could reach a logical conclusion by modelling the waves breaking on (a small part of) the shore using a free-surface RANS method, however this has not been demonstrated. Results for a single test case are provided for each of the covered methods, namely: the near-field waves, far-field waves at a constant depth (for both a straight course and curved path), and far-field waves within a region of variable water depth. The author concludes the paper by stating that comparisons with experiments are planned.

Most studies appear to assume that profiles of waves generated by fast ferries can be described by classical linear wave theory, however, Soomere et al. (2005) suggest that

this is not applicable with many of the long period waves when in shallow water and that a more appropriate model for long waves in shallow water is the Korteweg-de Vries (KdV) equation (cnoidal waves) which have more realistic, narrow crests and broad troughs than sine waves.

Soomere and Engelbrecht (2006) investigate events where considerable increases in wave amplitudes occur due to nonlinear superposition of solitary waves in shallow water. Such interactions have recently been proposed as an explanation for the generation of freak waves. The authors suggest that a suitable model for the description of the interaction of soliton-like shallow water waves travelling under slightly different directions is the Kadomtsev-Petviashvili (KP) equation.

Unsteady RANS simulations for a Wigley hull running at high speed in deep water and running at sub-critical speed in shallow water are presented by Sakamoto et al. (2007). Three types of investigations are made: (1) uncertainty analysis, (2) high-speed effect, and (3) shallow water effect. The resistance, pressure variation, wave pattern, boundary layer and vortices are studied. The present work is the first step toward the application of the URANS method to high-speed ship study. Free surface wave patterns at different Froude numbers clearly show the typical high-speed effect that a diverging wave dominates a transverse wave as Froude number is increased.

Some papers focus on the prediction of ship wash near the shore. Hong and Doi (2006) have developed a numerical method by using the interface capturing method and the Constrained Interpolation Profile (CIP) method. A comparison against experimental data shows the suitability of the prediction technique. The study has shown that the first wave run-up is the biggest of the first three waves, despite the height of the first wave being the lowest of the three when offshore. Erikson et al. (2005) describe a model to predict swash motion based on solutions to the nonlinear shallow

water equations to account for interaction between up-rush and back-wash at the still water shoreline and within the swash zone. The model was tested against wave groups representing vessel generated wave trains (run in a small wave basin). Accounting for swash interaction markedly improved results with respect to the maximum run-up length for cases with gentle foreshore slopes (but no improvement for steep slopes). In addition, an equation to predict the onset and degree of swash interaction including the effects of bed friction was developed.

Torsvik et al. (2006) and Torsvik (2006) investigate the passage through the trans-critical speed region of a moving ship in a shallow channel using numerical simulations based on a 1D version of forced Boussinesq equations. The transition is accomplished either by accelerating the ship in a region of constant depth or by moving the ship with constant speed over a sloping bathymetry. Results show that the generation of upstream solitary waves depends on time required for the transition, with large waves being generated for long transition times. It is also apparent that the shape of the wave pattern and the maximum amplitude of the waves differ significantly on whether the Froude number increases or decreases during the transition of the trans-critical region.

To determine the hull form parameters most affecting wake wash Robbins and Renilson (2006) created a systematic series of typical low wash-energy catamaran hull forms (consisting of a parent hull and six variants). A contemporary potential flow code (SHIPFLOW) was used to generate free surface elevations which were then analysed using a decay method. Regression analysis of the results helped to produce a simple prediction tool which the authors aimed to undertake early design assessments of particular hull forms. The regression analysis confirmed that the length on displacement (slenderness) and L/B ratios are the most dominant hull parameters.

9.4 Conclusions

The conclusions drawn by the 24th ITTC RC largely still hold. Notably, there is still a lack of appropriate benchmark data available in the public domain for researchers to undertake comparisons.

A common opinion is that it is still necessary to validate the numerical models in use based on experimental measurements (either/both model scale or in-situ) before they can be used for managing wake wash in a particular situation, regardless of what type of numerical model is deemed the most appropriate. As a result, the RC does not believe that enough experience presently exists to propose general guidelines for the prediction of far field waves and wash effects.

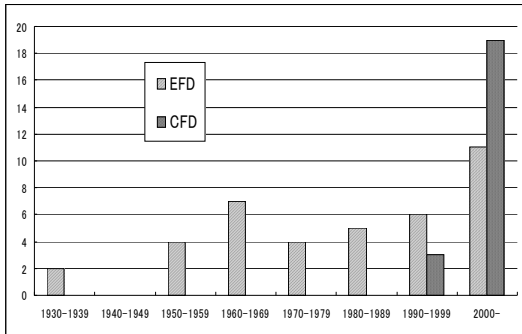
10. AIRWAKES

10.1 Introduction

This chapter reviews research efforts on ship airwakes. The ship airwake flow fields are characterized by strong bluff body shedding and subsequent evolution of the resulting vortex dominated flow field. In ship design, particular focus was initially on prediction of air pressure resistance and moments, flow field around ship superstructures including flume effects, and influence on maneuverability in strong wind conditions. More recently, interests are on the prediction and control of ship airwake and the interactions with aircraft, and effects of flow distortion created by the ship hull and superstructure on onboard anemometry. Since this is the first time to review the present topic, the following review starts with a historical overview. Then, past and ongoing EFD and CFD works are reviewed, and finally, recommendations for future work are given.



10.2 Historical Overview



As seen in the above figure, where number of reviewed papers is shown with respect to year periods, continuous effort on the present topic is reported in the past 80 years. No public reports were found in the period immediately before and after WW II. The first systematic study on a commercial ship, i.e., the cargo ship *London Mariner*, was reported in 1930 (Hughes, 1930). Before ca.1960, research interest was mainly on ships with particular superstructures, e.g., warships, bonito/tunny fishing boats, and train ferries.

In ca.1960 – ca.1970, more work was done for general commercial ships to investigate wind effects on maneuverability in strong wind conditions. In ca.1970 – ca.1990, when the world economy had to go through the *Oil Crises*, new challenges appeared in ship design, i.e., energy-saving design received more attention and better aerodynamic superstructure designs to yield low wind drags were investigated. The growth of experimental databases motivated investigation on more accurate methods to estimate wind force and moment.

In ca.1990 – ca.2000, the above studies were extended for modernized ship design, e.g., large tankers, LNG tankers, PCC ships, and modern aircraft carriers were new applications. Other new applications were detailed analysis of aerodynamic interactions between ship superstructure and aircraft (airplanes or helicopters), flume effects, and effects of flow around ship superstructures on anemometry. CFD works appeared in the late 1990s, and

increasing numbers of CFD studies are being reported, which is apparently due to the advancement of computer technology.

In the above-mentioned EFD studies, most investigations were carried out in wind tunnels, and very few were in water tanks, especially in the very early studies. The following sections give an overview of the past and ongoing EFD and CFD works, with more information presented for the more recent ongoing studies.

10.3 EFD Work, Modeling of Aerodynamic Forces, and New Applications

Early Work. As mentioned earlier, the first comprehensive and very systematic EFD work was reported by Hughes (1930), who presented systematic model tests made at the William Froude National Experiment Tank to investigate the wind force acting upon ships' superstructures. On the other hand, Izubuchi (1932) reported measurements of air resistance with models of the above-water portion of four typical warships in the wind tunnel at the Naval Research Institute. The study of Izubuchi (1932) was later extended for an airplane carrier advancing obliquely to the direction of wind.

In the 1950s, Araki and Hanaoka (1952) presented results for typical models of train ferries, and the data were used by Nakajima (1952) to investigate the effect of wind on the maneuverability of the same ships. In those days, another focus was on wind effects on maneuverability of relatively small ships with particular superstructures, e.g., fishing boats and small cargo ships. Such examples were seen in Kinoshita et al. (1954), who performed a series of wind tunnel experiments for a bonito/tunny fishing boat, and Okada (1957) who presented the results of wind-tunnel experiments for a small passenger ship and two fishing boats.

In the 1960s through 1970s, effort was directed toward very detailed wind tunnel measurements for other commercial ships: e.g.,

Kinoshita and Okada (1960) for cargo ships; Shearer (1961) for a tanker, two cargo ships, and a modernized passenger liner; Wanger (1967) for sixteen ship models including cargo ships, a passenger liner, a ferry, a fishing boat, and naval surface combatant; Aertssen and Colin (1968) for cargo ships and car-ferry; Tsuji et al. (1970) for large tankers, car carrier, container ship and fishing boats; and Aage (1971) for nine ship models including cargo ships, a tanker, a passenger liner, a ferry, and a fishing boat.

By using the data obtained in the above studies, many studies on modeling of aerodynamic forces and moments to develop empirical formula were initiated. For example, Isherwood (1972) proposed methods based on a linear multiple regression model for merchant ships, and by using the results, Inoue and Ishibashi (1972) investigated ship maneuverability and course stability. The status of the ongoing research in the 1970s was well summarized by Hamada (1983).

As ship design was modernized in the 1980s and 1990s, continuous efforts on developing EFD databases and modeling of aerodynamic forces and moments were made. For example, VLCC, PCC, and LNG became new applications. A method proposed in the wind engineering field was a straightforward application to ship superstructure design (e.g., a method proposed by Shiraishi et al., 1986). Approaches to solve equilibrium equations also appeared: e.g., Sezaki (1980) for a large car carrier; Tanaka et al. (1980) for a tanker, a container, and a car carrier; and Yoshimura and Nagashima (1985) for a car carrier. More comprehensive equilibrium equations were investigated, e.g., “a physical-mathematical model” proposed by Yoneta et al. (1992) who considered six elements of fluid dynamic forces and stall effects in association with six non-dimensional hull parameters.

More Recent Work. In the 1990s, EFD techniques were more advanced, and more realistic and complex wind and ship conditions

were considered, e.g., Blendermann (1995) performed wind-tunnel measurements in non-uniform airflow and proposed a method to estimate the wind loading of ships. Other examples are seen in Fujiwara et al. (1998) who carried out very detailed measurements and proposed a method to estimate wind forces; Nimura et al. (1997) who focused on a tanker in ballast condition and performed wind tunnel tests not only for forces but for flow visualization; and Yamano and Saito (1997) who proposed a practical method based on a small number of data.

An attempt to reduce wind force on ship super structures was presented by Matsumoto et al. (2003), who confirmed their success by wind tunnel measurements and reported a reduction of wind resistance for a Bulk Carrier of about 10%, side wind force and yaw moment for a PCC of about 20%, and the estimated total reduction of horsepower for PCC in a case of about 6%. Kulkarni et al. (2005) conducted an experimental study of the flow field over a simplified superstructure of a ship with two funnels ejecting iso-thermal exhaust, and presented very detailed measurements which will be applicable for CFD validation.

New Applications. In the 2000s, new applications appeared, i.e., prediction and control of ship airwakes and the interactions with aircraft (airplanes or helicopters), for which the motivations were mainly from naval applications. Specific requirements for design, flow, and measurements were described by Carico (2004), Bradley et al. (2005), and Platt (1998). There is an interest on the influences of a ship airwake on aircraft operating nearby, and the reduction of both turbulence levels and downwash velocities in the ship airwake, which should improve pilot workload and helicopter performance. Wind tunnel experiments have been a major approach for the ongoing research.

Derby and Yamauchi (2003) performed wind tunnel measurements for 1/48th-scale



rotorcraft models and an amphibious assault ship model, in order to investigate ship/rotorcraft interaction and the aerodynamic interaction of rotorcraft with other aircraft, with large structures, and with the ground. Silva et al. (2004) presented the design and execution of a small-scale wind tunnel investigation of V-22 shipboard interactional aerodynamic phenomena. Landman et al. (2005) conducted an experimental study with particle image velocimetry measurements to evaluate the effectiveness of deck-edge columnar vortex generators on aircraft carriers.

Shafer and Ghee (2005) presented a study of active and passive flow control over the flight decks of small naval vessels. A 1:144 scale model of the U.S. Navy destroyer DDG-81 was used to explore the problems related to unsteady flow fields and large mean velocity gradients of ship airwakes, which cause excessive pilot workloads for helicopter operations in the vicinity of small naval surface vessels. With the same objectives, Greenwell and Barrett (2006) investigated inclined screens for the control of ship airwakes, and presented results from a wind tunnel investigation of flow control devices applied to a generic frigate flight-deck.

Findlay and Ghee (2006) presented an experimental investigation of ship airwake flow control for a US navy flight II-A class destroyer (DDG), with the main objective to augment and improve airflow over a ship top-side geometry. A test was conducted with flow control devices fixed to an existing wind tunnel model of a 1/144th scale DDG-81 hull form with wind straight down the bow.

10.4 CFD Work and Experimental Validation

CFD work on ship airwakes was initiated in the late 1990s. In the 2000s, the number of reports rapidly increased, which is clearly due to the advent of powerful computational environments. Initially, numerical models and

geometry were relatively simple, and later these were considerably more complex and comprehensive. Most work focused on prediction of flow rather than aerodynamic forces, and some were associated with wind-tunnel experiments to validate the numerical results.

Applications cover naval ships, commercial and research ships. For naval ships, a main interest follows that of the earlier-mentioned EFD work, i.e., prediction and control of ship airwakes and the interactions with aircraft. For commercial and research ships, the interest is on the effects of flow distortion created by the ship hull and superstructure on onboard anemometry. In the following, these are separately reviewed, i.e., for naval ship applications, and for merchant and research ship applications.

Applications for Naval Ships. Liu et al. (1998) presented a numerical method to simulate ship airwake flow fields. The method is based on coupling of steady and unsteady solution schemes, and the results were presented for a generic frigate shape. Bogstad et al. (1999) performed CFD for Navy ships by using an inviscid flow solver. The objective was development of a ship airwake aerodynamic database to be used and integrated into a helicopter flight simulator. Reddy et al. (2000) simulated turbulent flow around a generic frigate shape. A commercial CFD code, FLUENT, was used in the study and results were compared with wind-tunnel flow visualization data.

Sharma and Long (2001) and Sezer-Uzol et al. (2005) presented their continuous effort on simulating flow over the San Antonio class LPD 17 ship. The numerical method is based on an unstructured finite-volume inviscid scheme. In their work, the most recent focus was on capturing the massively separated flow from sharp edges of blunt bodies. CFD analysis for the same ship was also done by Ramamurti and Sandberg (2002) and Camelli et al. (2003) by using their finite-volume unstructured CFD

code. Camelli et al. investigated temperature associated with gas dynamics, and the study was extended for another ship, a naval transport ship TAKE 1, by using Very Large Eddy Simulation (VLES) (Camelli et al., 2004).

Bunnell (2001) presented a time-varying ship airwake model around a LHA ship. The model was developed by using their CFD scheme together with a blade-element model of a helicopter in order to represent the complex interactions between the rotorcraft and the turbulent field. A similar topic was also investigated by WakeField et al. (2002), who focused more on development of a CFD model of a hovering helicopter main rotor. The airwake around a TTCP simple frigate ship was considered, and a wind-tunnel EFD study was also done to validate the numerical results.

Polsky (2002) and Czerwiec and Polsky (2004) used a NS solver to simulate the unsteady flow field produced by the superstructure of a LHA-class US Navy ship. Particular focus was on the effectiveness of the bow flap, and wind-tunnel experiments were also performed to validate their numerical results. Syms (2003, 2004) also performed a CFD study on the airwake around a simplified frigate shape (SFS). Initially, CFD based on a lattice Boltzmann algorithm was applied to SFS 1 ship, and later, a CFD based finite-volume scheme with $k-\epsilon$ turbulence model was applied to a simplified Halifax-Class Canadian Patrol Frigate (CPF) model. The former results were compared with wind-tunnel measurements.

Most recently, CFD applications have been extended for superstructure design, sensitivity analysis of modeling parameters, and detailed validation of CFD results through comparison with measurements. For example, papers were presented by Nangia and Lumsden (2004) for CFD work on Columnar Vortex Generators (CVG) to control airwakes over flight decks of large aircraft carriers; Rajagopalan et al. (2005) for EFD and CFD works on simulation of $1/48^{\text{th}}$ -scale amphibious assault ship; and

Arunajatesan et al. (2004) and Shipman et al. (2005) for EFD and CFD work investigating the sensitivity of the airwake solution to several modeling parameters, including geometric complexity and the resolution of boundary layers.

Applications for Merchant and Research Ships.

In contrast to naval applications, reports were fewer, but several noteworthy CFD works were presented for merchant and research ships. The main interest rests on effects of flow distortion created by the ship hull and superstructure and the influences on onboard wind measurements. Futatsudera et al. (2002) analyzed the ship airwake around a simplified Japan Coast Guard patrol boat *Soya* by using a commercial CFD code, FLUENT, and the results were validated through comparison with $1/50^{\text{th}}$ -scale model measurements. Popinet et al. (2004) used a time-dependent Large Eddy Simulation numerical technique to investigate the effect of the research vessel *Tangaroa* on both the mean and turbulent characteristics of airflow. The numerical results were compared with onboard measurements.

On the other hand, Moat et al. (2006a, 2006b) was motivated to investigate wind speed bias due to flow distortion in wind speed reports from voluntary observing ships (VOS). First, their CFD code based on a finite-volume RANS solver was applied to the research ship RRS *Charles Darwin* and the results were compared with the onboard measurements; next, the CFD method was applied to examine the airflow above the bridge of a typical, or generic, tanker/ bulk carrier/ general cargo ship. They reported that the wind speed bias is highly dependent upon the anemometer location and varies from accelerations of 10% or more to decelerations of 100%. The wind speed bias at particular locations also varies with the relative wind direction, that is, the angle of the ship to the wind.



10.5 Conclusion

For the first time, the 25th ITTC RC reviewed past and ongoing research on ship airwakes. Continuous effort on EFD and CFD works is reported in the past 80 years. Until recently, EFD has played a major role on the prediction of aerodynamic forces, while CFD is mainly used for prediction of flow fields. With the recent advancements of high-performance computers, CFD will become a more practical method in the near future, but needs more complete validation work. Due to the complexity of flow associated with ship airwakes, CFD and EFD must be used in a complementary manner.

As reviewed earlier, most of the latest work on ship airwakes is motivated by naval applications, in which the design problem of very complex ship superstructures is involved. Approaches based on both EFD and CFD have been very promising, therefore, more future study must be focused on new approaches for new ship concepts, e.g., high-speed and Multi-hull ships.

11. RECOMMENDATIONS

Adopt the updated procedure No. 7.5-01-01-01 Ship Models.

Adopt the updated procedure No. 7.5-02-02-01 Resistance Tests.

12. REFERENCES

- Aage, C., 1971, "Wind Coefficients for Nine Ship Models," Hydro and aerodynamics laboratory Report, No.A-3.
- Aertssen, G. and Colin, P.E., 1968, "Wind Tunnel Tests on a Model of a Car-ferry," I.S.P., Vol.15, No.163, pp. 71-77.
- Alexandrov, N.M. and Lewis, R.M., 2002, "An Overview of First-Order Model Management for Engineering Optimization", Optimization and Engineering, Vol. 2 (4), 413-430.
- Ando, J., Yoshitake, A. and Nakatake, K., 2005, "Numerical and Experimental Studies on Wavemaking Resistance of Catamaran and Trimaran," Proc. 5th Osaka Colloquium, Osaka, Japan.
- Araki, H. and Hanaoka, T., 1952, "Wind Tunnel Experiments on Train Ferries," J. Society of Naval Architects of Japan, No. 84, pp 61-79.
- Arunajatesan, S., Shipman, J. D., Sinha, N., 2004, "Towards Numerical Modeling of Coupled VSTOL-ship Airwake Flowfields," AIAA-2004-0052.
- Atsavaprane P., Forlini T., Furey D., Hamilton J., Percival S., Sung C.H., 2004, "Experimental Measurement for CFD Validation of the Flow about a Submarine(ONR-Body 1)", Proc. 25th Symposium on Naval Hydrodynamics, St. John's, Newfoundland & Labrador, Canada.
- Baik S., Vlachogiannis M., and Hanratty T.J., 2005, "Use of Particle Image Velocimetry to Study Heterogeneous Drag Reduction", Experiments in Fluids, Vol. 39, pp. 637-650.
- Balzerek, H. and Koslowski, J., 2007, "Ship-induced Riverbank and Harbour Damage", Hydro International, September.
- Bandyopadhyay P.R., Henoeh C., Hrubes J.D., Semenov B.N., Amirov A.I., Kulik V.M., Malyuga A.G., Choi K.S., and Escudier M.P., 2005, "Experiments on the Effects of Aging on Compliant Coating Drag Reduction", Physics of Fluids, Vol. 17, Art. No. 085104.
- Bensow, R. E., Fureby, C., Liefvendahl, M. and Persson, T., 2006, "A Comparative Study of RANS, DES and LES," Proc. 26th Symp. Naval Hydrodynamics, Rome, Italy.

- Bertram, V. (Ed.), 2007, 10th Numerical Towing Tank Symposium, 23-25 September, Hamburg, Germany.
- Besnard E., Schmitz A., Hefazi H., and Shinde R., 2007, "Constructive Neural Networks and their Application to Ship Multi-Disciplinary Design Optimization", J. Ship Research, Vol. 51 (1).
- Bhushan, S., Xing, T., Carrica, P. and Stern, F., 2007, "Model- and Full-Scale URANS/DES Simulations for Athena R/V Resistance, Powering, and Motions," Proc. 9th Int. Conf. Numerical Ship Hydrodynamics, Ann Arbor, MI, USA.
- Blendermann, W., 1995, "Estimation of Wind Loads on Ships in Wind with a Strong Gradient," OMAE, Vol.1-A, pp. 271-277.
- Bogstad, M.C., Ait-Ali-Yahia, D., Metcalfe, L., Habash, W.G., Giannias, N., Longo, V., 1999, "CFD Ship Airwake Analysis for Helicopter Flight Simulators," AIAA 99-0996.
- Bradley, R., Macdonald, C.A., Buggy, T.W., 2005, "Quantification and Prediction of Pilot Workload in the Helicopter/Ship Dynamic Interface," Proc. IMechE Vol. 219 Part G: J. Aerospace Engineering, pp. 429-443.
- Brandt, T., 2007, "Study on Numerical and Modelling Errors in LES Using a Priori and a Posteriori Testing", Doctoral dissertation, Helsinki University of Technology, Department of Mechanical Engineering, Espoo, Finland.
- Bunnell, J.W., 2001, "An Integrated Time-Varying Airwake in a UH-60 Black Hawk Shipboard Landing Simulation," AIAA-2001-4065.
- Camelli, F., Soto, O., Lohner, R., Sandberg, W.C., Ramamurti, R., 2003, "Topside LPD17 Flow and Temperature Study with An Implicit Monolithic Scheme," AIAA-2003-0969.
- Camelli, F., Lohner, R., Sandberg, W.C., Ramamurti, R., 2004, "VLES Study of Ship Stack Gas Dynamics," AIAA-2004-0072.
- Campana E.F., Peri D., Tahara Y. and Stern F., 2006, "Shape Optimization in Ship Hydrodynamics using Computational Fluid Dynamics", Computer Methods in Applied Mechs. and Engineering, Vol. 196, 634-651.
- Carico, D., 2004, "Rotorcraft Shipboard Flight Test Analytic Options," Proc. 2004 IEEE Aerospace Conference, pp. 2988-2998.
- Carrica, P. M., Wilson, R. V., Noack, R., Xing, T., Kandasamy, M., Shao, J., Sakamoto, N. and Stern, F., 2006, "A Dynamic Overset, Single-Phase Level Set Approach for Viscous Ship Flows and Large Amplitude Motions and Maneuvering," Proc. 26th Symp. Naval Hydrodynamics, Rome, Italy.
- Cea L., Puertas J., and Pena L., 2007, "Velocity Measurements on Highly Turbulent Free Surface Flow using ADV", Experiments in Fluids, Vol. 42, pp. 333-348.
- Cebeci, T., 2004, "Analysis of Turbulent Flows (Second Revised and Expanded Edition)," Elsevier.
- Celik, I., Li, J., Hu, G. and Shaffer, C., 2005a, "Limitations of Richardson Extrapolation and some Possible Remedies," Journal of Fluids Engineering, Vol. 127, pp.795-805.
- Celik, I.B., Cehreli, Z.N. and Yavuz I., 2005b, "Index of Resolution Quality for Large Eddy Simulations," Journal of Fluids Engineering, Vol. 127, pp. 949-958.
- Chalkias, D.S. and Grigoropoulos, G.J., 2005, "Wash Effects of High-Speed Monohulls", International Conference on Fast Sea Transportation (FAST 2005).



- Chalkias, D.S. and Grigoropoulos, G.J., 2007, "Experimental Investigations of the Waves Generated by High-Speed Ferries", International Conference on Fast Sea Transportation (FAST 2007).
- Chen J.H. and Chang C.C., 2006, "A Moving PIV System for Ship Model Test in a Towing Tank", Ocean Engineering, Vol. 33, pp. 2025–2046.
- Chen P.F, Huang C.H., Fang M.C. and Chou J.H., 2006, "An Inverse Design Approach in Determining the Optimal Shape of Bulbous Bow With Experimental Verification", J. Ship Research, Vol. 50 (1), 1-14.
- Choi, J-K., Hsiao, C-T. and Chahine, G. L., 2006, "Design Trade-Off Analysis for High Performance Ship Hull with Air Plenums," 2nd Int. Symp. Seawater Drag Reduction, Busan, Korea.
- Choi, J-K., Hsiao, C-T. and Chahine, G. L., 2007, "Numerical Studies on the Hydrodynamic Performance and the Startup Stability of High Speed Ship Hulls with Air Plenums and Air Tunnels," Proc. 9th Int. Conf. Fast Sea Transportation, FAST2007, Shanghai, China.
- Coles, D.E., 1987, "In Perspectives in Turbulence Studies," Springer.
- Czerwiec, R.M., Polsky, S.A., 2004, "LHA Airwake Wind Tunnel and CFD Comparison with and without Bow Flap," AIAA-2004-4832.
- Derby, M.R., Yamauchi, G.K., 2003, "Design of 1/48th-scale Models for Ship/Rotorcraft Interaction Studies," AIAA-2003-3952.
- Deutsch S., Fontaine A.A., Moeny M. J., and Petrie H. L., 2006, "Combined Polymer and Microbubble Drag Reduction on a Large Flat Plate", Journal of Fluid Mechanics, Vol. 556, pp. 309-327.
- Di Mascio, A., Broglia, R. and Muscari, R., 2007, "On the Application of the Single-Phase Level Set Method to Naval Hydrodynamic Flows," Computers & Fluids, Vol. 36, pp. 868 – 886.
- Doctors, L.J. and Scrace R.J., 2003, "The Optimization of Trimaran Sidehull Position for Minimum Resistance", FAST 2003, Ischia, Italy
- Dommermuth, D. G., O'Shea, T. T., Wyatt, D. C., Sussman, M., Weymouth, G. D., Yue, D. K. P., Adams, P., and Hand, R., 2006, "The Numerical simulation of Ship Waves Using Cartesian-Grid and Volume-of-Fluid Methods," Proc. 26th Symp. Naval Hydrodynamics, Rome, Italy.
- Dommermuth, D. G., O'Shea, T. T., Wyatt, D. C., Ratcliffe, T., Weymouth, G. D., Hendrikson, K. L., Yue, D. K. P., Sussman, M., Adams, P. and Valenciano, M., 2007, "An Application of Cartesian-Grid and Volume-of-Fluid Methods to Numerical Ship Hydrodynamics," Proc. 9th Int. Conf. Numerical Ship Hydrodynamics, Ann Arbor, MI, United States.
- Eca, L. and Hoekstra, M., 2002, "An Evaluation of Verification Procedures for CFD Applications," Proc. 24th Symposium on Naval Hydrodynamics, Fukuoka, Japan.
- Eca, L. and Hoekstra, M. (Eds.), 2004, Workshop on CFD Uncertainty Analysis, Lisbon, Portugal.
- Eca, L. and Hoekstra, M., 2005, "On the Influence of Grid Topology on the Accuracy of Ship Viscous Flow Calculations," Proc. 5th Osaka Colloquium, Osaka, Japan.
- Eca, L. and Hoekstra, M., 2006a, "An Introduction to CFD Code Verification Including Eddy-Viscosity Models," ECCOMAS CFD 2006, TU Delft, The Netherlands.

- Eca, L. and Hoekstra, M., 2006b, "Verification of Turbulence Models with a Manufactured Solution," ECCOMAS CFD 2006, TU Delft, The Netherlands.
- Eca, L. and Hoekstra, M., 2006c, "On the Influence of the Iterative Error in the Numerical Uncertainty of Ship Viscous Flow Calculations," Proc. 26th Symposium on Naval Hydrodynamics, Rome, Italy.
- Eca, L. and Hoekstra, M. (Eds.), 2006d, 2nd Workshop on CFD Uncertainty Analysis, Lisbon, Portugal.
- Erikson, L.H., Larson, M. and Hanson, H., 2005, "Prediction of Swash Motion and Run Up including the Effects of Swash Interaction", Coastal Engineering, Vol. 52.
- Felli M. and Felice F.D., 2005, "Propeller Wake Analysis in Nonuniform Inflow by LDV Phase Sampling Techniques", Journal of Marine Science and Technology, Vol. 10, pp. 159–172.
- Ferrante A. and Elghobashi S., 2005, "Reynolds Number Effect on Drag Reduction in a Microbubble-Laden Spatially Developing Turbulent Boundary Layer," Journal of Fluid Mechanics, Vol. 543, pp. 93–106 .
- Findlay, D.B., Ghee, T., 2006, "Experimental Investigation of Ship Airwake Flow Control for a US Navy Flight II-A Class Destroyer (DDG)," AIAA-2006-3501.
- Foeth E.J., van Doorne C.W.H., van Terwisga T., and Wieneke B., 2006, "Time Resolved PIV and Flow Visualization of 3D Sheet Cavitation", Experiments in Fluids, Vol. 40, pp. 503–513.
- Fu T.C., Fullerton A.M., Terrill E., and Lada G., 2006, "Measurements of the Wave Field Around the R/V Athena I", Proc. 26th Symposium on Naval Hydrodynamics, Rome, Italy.
- Fujiwara T., Ueno, M., Nimura, T., 1998, "Estimation of Wind Forces and Moments acting on Ships," J. Society of Naval Architects of Japan, No. 183, pp. 77-90.
- Futatsudera, A., Miyazono, D., Moriuchi, Y., Yamaguchi, H., Kawamura T., Miyanaga, M., 2002, "Influence of the Ship and Superstructure on the on Board Measurement of Wind and Turbulence," J. Society of Naval Architects of Japan, Vol. 192, pp. 71-80.
- Gano, S.E., Renaud, J.E. and Sandersz, B., 2004, "Variable Fidelity Optimization Using a Kriging Based Scaling Function", 10th AIAA/ISSMO Multidisciplinary Analysis and Optimization Conf., Albany, New York
- Goel, T., Haftka, R.T., Shyy, W. and Queipo, N.V., 2007, "Ensemble of Surrogates", Struct Multidisc Optim., Vol. 33, 199–216
- Gorski, J. J., Ebert, M. P. and Mulvihill, L., 2007, "Uncertainties in the Resistance Prediction of Underwater Vehicles," NATO AVT Symp. Computational Uncertainty in Military Design, Athens, Greece.
- Greenwell, D.I., Barrett, R.V., 2006, "Inclined Screens for Control of Ship Air Wakes," AIAA-2006-3502.
- Grigson, C.W.B., 1993, "An Accurate Smooth Friction Line for Use in Performance Prediction," Trans. RINA Part A, Vol. 135, pp. 149-162.
- Gumbert, C.R., Newman, P.A. and Hou, J.W., 2005, "High-Fidelity Computational Optimization for 3-D Flexible Wings: Part II - Effect of Random Geometric Uncertainty on Design", Optimization and Engineering, Vol. 6 (1), 139-156.
- Hamada, N., 1983, "Wind Pressure of Superstructure," Senpaku, Vol. 56, No.5, pp. 26-32.



- Hanjalic, K., 2005, "Will RANS Survive LES? A View of Perspectives," J. of Fluids Engineering, Vol. 127, pp. 831 – 839.
- Hino, T. (Ed.), 2005, CFD Workshop Tokyo 2005, March 9-11, Tokyo, Japan.
- Hino, T., 2006, "CFD-Based Estimation of Propulsive Performance in Ship Design," Proc. 26th Symp. Naval Hydrodynamics, Rome, Italy.
- Hino, T., Kobayashi, H., and Takeshi, H., 2007, "CFD-Based Design of Ship Hull Forms with Azimuth Propulsion System," Proc. 9th Int. Conf. Numerical Ship Hydrodynamics, Ann Arbor, MI, (USA).
- Hofmann, H., Lorke, A. and Peters, F., 2008, "The Relative Importance of Wind and Ship Waves in the Littoral Zone of a Large Lake," Limnol. Oceanogr., 53(1), pp. 368 – 380.
- Hong C.B. and Doi, Y., 2006, "Numerical and Experimental Study on Ship Wash Including Wave-Breaking on Shore", Journal of Waterway, Port, Coastal and Ocean Engineering, ASCE, Sept/Oct.
- Hoyer K., Holzner M., Lu"thi B., Guala M., Liberzon A., and Kinzelbach W., 2005 "3D Scanning Particle Tracking Velocimetry", Experiments in Fluids, Vol. 39, pp. 923–934.
- Huan, J. C. and Huang, T. T., 2007, "Surface Ship Total Resistance Prediction Based on a Nonlinear Free Surface Potential Flow Solver and a Reynolds-Averaged Navier-Stokes Viscous Correction," J. Ship Research, Vol. 51, pp. 47 – 64.
- Huang, D., Allen, T.T., Notz, W.I. and Miller, R.A., 2006, "Sequential Kriging Optimization Using Multiple-Fidelity Evaluations", Struct Multidisc Optim., Vol. 32, 369–382.
- Hughes G., 1930, "Model Experiments on the wind Resistance of Ships," T.I.N.A. Vol. 35, pp. 310-329.
- Hughes, G., 1952, "Frictional Resistance of Smooth Plane Surface in Turbulent Flow - New Data and Survey of Existing Data-," Trans I. N. A.
- IEEE-SIS IEEE Swarm Intelligence Symposium, 2006, Proceedings, Indianapolis, Indiana (USA).
- Inoue, S., Ishibashi, Y., 1972, "The Effects of Wind on The Ship Manoeuvrability (I)," J. West-Japan Society of Naval Architects, No. 44, pp. 111-128.
- Isherwood, R.M., 1972, "Wind Resistance of Merchant Ships," The Royal Institute of Naval Architects, Vol.115, pp. 327-338.
- Izubuchi, T., 1932, "Model Experiments on the Air Resistance of Warships," J. Soc. Naval Architects of Japan, No. 49, pp. 129-151.
- Jin, R., Chen, W. and Simpson T.W., 2001, "Comparative Studies of Metamodeling Techniques Under Multiple Modeling Criteria", Struct. Multidisc. Optim., Vol. 23, 1-13.
- Jordan, S.A., 2005, "A Priori Assessments of Numerical Uncertainty in Large-Eddy Simulations," Journal of Fluids Engineering, Vol. 127, pp. 1171-1182.
- Joslin R.D., Thomas R.H., and Choudhari M.M., 2005, "Synergism of Flow and Noise Control Technologies", Progress in Aerospace Sciences, Vol. 41, pp. 363-417.
- Jovanovic J., Pashtropanska M., Frohnapfel B., Durst F., Koskinen J., and Koskinen K., 2006, "On the Mechanism Responsible for Turbulent Drag Reduction by Dilute addition of High Polymers: Theory, Experiments, Simulations, and Predictions", ASME Journal of Fluids Engineering, Vol. 128, pp. 118-130.

- Jung K.H., Chang K.-A., and Huang E.T., 2005, "Two-Dimensional Flow Characteristics of Wave Interactions with a Free-Rolling Rectangular Structure", Ocean Engineering, Vol. 32, pp. 1–20.
- Jung K.H., Chang K.-A., and Jo H.J., 2006, "Viscous Effect on the Roll Motion of a Rectangular Structure", ASCE Journal of Engineering Mechs., Vol. 132, pp. 190–200.
- Jung K.H., Kim K.C., Yoon S.Y., Kwon S.H., Chun H.H., and Kim M.C., 2006, "Investigation of Turbulent Flows in a Waterjet Intake Duct Using Stereoscopic PIV Measurements", J. Marine Science and Technology, Vol. 11, pp. 270–278.
- Karion A., Fu T.C., Rice J.R., Walker D.C., and Furey D.A., 2004, "Experimental Measurements of the Surface of a Breaking Bow wave", Proc. 25th Symposium on Naval Hydrodynamics, St. John's, Newfoundland and Labrador, Canada.
- Katsui, T., Asai, H., Himeno, Y., Tahara, Y., 2005, "The Proposal of a New Friction Line," Proc. 5th Osaka Colloquium on Advanced Research on Ship Viscous Flow and Hull Form Design by EFD and CFD Approaches, Osaka, Japan, pp. 76-83.
- Kim, J., Paterson, E.G., Stern, F., 2006, "RANS Simulation of Ducted Marine Propulsor Flow Including Subvisual Cavitation and Acoustic Modeling," Journal of Fluids Engineering, Vol. 128, pp. 799-810.
- Kim, J. and Bewley, T.R., 2007, "A Linear Systems Approach to Flow Control," Annual Review of Fluid Mechanics, Vol. 39, pp. 383-417.
- Kim, S-E and Cokljat, D., 2007, "Evaluation of an URANS-LES Hybrid Approach for Turbulent Free Surface Flows around Surface-Piercing Bodies," Proc. 9th Int. Conf. Numerical Ship Hydrodynamics, Ann Arbor, MI, United States.
- Kim, K. S., Kim, J., Park. I. R., Kim, G. D. and Van, S. H., 2007, "RANS Analysis for Hull-Propeller-Rudder Interaction of a Commercial Ship by Using the Overset Grid Scheme," Proc. 9th Int. Conf. Numerical Ship Hydrodynamics, Ann Arbor, MI, United States.
- Kinoshita, M., Hanaoka, T., Nakajima, Y., 1954, "On the Wind Effect on the Manoeuverability of a Bonito & Tunny Fishing Boat," J. Society of Naval Architects of Japan, No.86, pp 317-331.
- Kinoshita, M., Okada, S., 1960, "On the Wind Pressure of Superstructure," Senapaku, Vol. 35, No.11, pp. 101-111.
- Kitagawa A., Hishida K., and Kodama Y., 2005, "Flow Structure of Microbubble-Laden Turbulent Channel Flow Measured by PIV Combined with the Shadow Image Technique", Experiments in Fluids, Vol. 38, pp. 466-475.
- Kodama Y., Takahashi T., Makino M. and Ueda T., 2004a, "Conditions for Microbubbles as a Practical Drag Reduction Device for Ships," Proc. 5th International Conference on Multiphase Flow, Yokohama, Japan, Paper No. 535.
- Kodama Y., Takahashi T., Hori T., Makino M. and Ueda T., 2004b, "Characteristics of Microbubble Drag Reduction on a 50m-long Flat Plate," Proc. 3rd International Symposium on Two-Phase Flow Modelling and Experimentation, Pisa, Italy
- Kodama Y., Murai Y., Kawamura T., Sugiyama K. and Yamamoto, F., 2006, "Direct Comparison of Experimental and Numerical Simulation on Microbubble Flows for Skin Friction Reduction", Proc. 26th Symposium on Naval Hydrodynamics, Rome, Italy.
- Kolda, T.G., Lewis, R.M. and Torczon V., 2003, "Optimization by Direct Search: New



- Perspectives on Some Classical and Modern Methods”, SIAM review, Vol. 45 (3), 385-482.
- Kulkarni, P.R., Singh, S., Seshadri, V., 2005, “Experimental Study of the Flow Field Over Simplified Superstructure of a Ship,” Int. J Maritime Eng, IJME Part A3, pp. 19-42.
- Kumar, S.A., Heimann, J., Hutchison, B.L. and Fenical, S.W., 2007, “Ferry Wake Wash Analysis in San Francisco Bay”, Ports 2007 Conference, ASCE, San Diego, USA.
- Kunz R.F., Gibeling H.J., Maxey M.R., Tryggvason G, Fontaine A.A., Petrie H.L., and Ceccio S.L., 2007, “Validation of Two-Fluid Eulerian CFD Modeling for Microbubble Drag Reduction across a wide Range of Reynolds Numbers”, Journal of Fluids Engineering, Vol. 129, pp. 66-79.
- Landman, D., Lamar, J.E., Swift, R., 2005, “Particle Image Velocimetry Measurements to Evaluate the Effectiveness of Deck-Edge Columnar Vortex Generators on Aircraft Carriers,” RTO MP AVT-124 No.8, Presented at the AVT Symposium, pp.7-1 - 7-16 465.
- Lazauskas, L., 2007, “The Hydrodynamic Resistance, Wave Wakes and Bottom Pressure Signatures of a 5900t Displacement Air Warfare Destroyer”, <http://www.cyberiad.net/wakepredict.htm>, accessed 12 February 2008.
- Lee, S.J. and Kang, J.H., 2006, “Development of a Pressure Sensitive Paint Technique for Low-Speed Flows and Its Application”, J. of Visualization, Vol. 9, pp. 137-144.
- Lee S.J., Paik B.G., and Lee C.M., 2005, “Phase-Averaged Particle Tracking Velocimetry Measurements of Propeller Wake”, Journal of Ship Research, Vol. 49, pp. 43–54.
- Leroyer, A., Hay, A., Queutey, P. and Visonneau, M., 2005, “Free-Surface RANSE Simulations for Moving Bodies with Adaptive Mesh Refinement,” Proc. 5th Osaka Colloquium, Osaka, Japan.
- Liu, J., Long, L.N., Modi, A., 1998, “Higher Order Accurate Solutions of Ship Airwake Flow Fields Using Parallel Computer,” The American Helicopter Society 54th Annual Forum, Washington DC.
- Lyakhovitsky, A., 2007, “Shallow Water and Supercritical Ships”, Backbone Publishing Company.
- Macfarlane, G.J., 2006, “Correlation of Prototype and Model Wave Wake Characteristics at Low Froude Numbers”, RINA Transactions, Part A2, International Journal of Maritime Engineering.
- Macfarlane, G.J., 2008, “Correlation of Prototype and Model Wave Wake Characteristics of a Catamaran”, SNAME Marine Technology (to appear).
- Macfarlane, G.J. and Cox, G., 2004, “The Development of Vessel Wave Wake Criteria for the Noosa and Brisbane Rivers in Southeast Queensland”, Fifth Int. Conf. on Coastal Environment 2004 - Environmental Problems in Coastal Regions.
- Macfarlane, G.J. and Cox, G., 2007, “An Introduction to the Development of Rational Criteria for Assessing Vessel Wash Within Sheltered Waterways”, IMarEST Journal of Marine Design and Operations.
- Macfarlane, G.J., Cox, G. and Bradbury, J., 2008, “Bank Erosion from Vessel Wash in Sheltered Waterways”, RINA Transactions, Part B, International Journal of Small Craft Technology (to appear).
- Maki, K. J., Doctors, L. J., Rhee, S. H., Wilson, W. M., Beck, R. F. and Troesch, A. W., 2007, “Resistance Predictions for a High-

- Speed Sealift Trimaran,” Proc. 9th Int. Conf. Numerical Ship Hydrodynamics, Ann Arbor, MI, USA.
- Martinelli, L. and Jameson, A., 2007, “An Adjoint Method for Design Optimization of Ship Hulls”, 9th Int. Conf. on Numerical Ship Hydrodynamics, Ann Arbor (USA).
- Martins, J., Alonso, J.J., Reuther, J.J., 2005, “A Coupled-Adjoint Sensitivity Analysis Method for High-Fidelity Aero-Structural Design”, Optimization and Engineering, Vol. 6 (1), 33-62.
- Mason, A. and Thomas, G., 2007, “Stochastic Optimisation of IACC Yachts”, 6th Int. Conf. on Computer Applications and Information Technology in the Maritime Industries (Compit’07), Cortona (Italy), 122-141.
- Matsumoto, K., Tanaka, Y., Hirota, K., Usami, S., Takagishi, K., 2003, “Reduction of Wind Forces acting on Ships,” J. Kansai Society of Naval Architects, Japan, No.240, pp. 115-121.
- Mattson, C.A. and Messac, A., 2005, “Pareto Frontier Based Concept Selection Under Uncertainty, with Visualization”, Optimization and Engineering, Vol. 6 (1), 33-62.
- McGraw C.M., Bell J.H., Khalil G., and Callis J.B., 2006, “Dynamic Surface Pressure Measurements on a Square Cylinder with Pressure Sensitive Paint”, Experiments in Fluids, Vol. 40, pp. 203–211.
- Meng, J., 2005, “Sea Water Drag Reduction & World Peace,” Presentation at the 2nd International Symposium on Seawater Drag Reduction, Busan, Korea.
- Miller, R., Gorski, J., Xing, T., Carrica, P. and Stern, F., 2006, “Resistance Predictions of High Speed Mono and Multihull Ships with and without Water Jet Propulsors using URANS,” Proc. 26th Symp. Naval Hydrodynamics, Rome, Italy.
- Millward A. and Brown G.L., 2005, “The Capacitance Method of Measuring the Wetted Surface Area of a Ship Model”, International Shipbuilding Progress, Vol. 52, pp. 231-244.
- Min T., Kang S.M., Speyer J.L., and Kim J., 2006, “Sustained Sub-Laminar Drag in a Fully Developed Channel Flow”, Journal of Fluid Mechanics, Vol. 558, pp. 309-318.
- Mittal, R. and Iaccarino, G., 2005, “Immersed Boundary Methods,” Ann. Rev. Fluid Mechanics, Vol. 37, pp. 239 – 261.
- Moat, B.I., Yelland, M.J., Pascal, R.W., 2006a, “Quantifying the Airflow Distortion over Merchant Ships. Part I: Validation of a CFD Model,” J. Atmospheric and Oceanic Technology, Vol. 23, pp. 341-350.
- Moat, B.I., Yelland, M.J., Anthony, F., Molland, A.F., 2006b, “Quantifying the Airflow Distortion over Merchant Ships. Part II: Application of the Model Results,” J. Atmospheric and Oceanic Technology, Vol. 23, pp. 351-360.
- Moore K.J., Moore C.M, Stern M.A., and Deutsch S., 2006, “Design and Test of a Polymer Drag Reduction System on Sea Flyer”, Proc. 26th Symposium on Naval Hydrodynamics, Rome, Italy.
- Murai Y., Fukuda H., Shi Y., Kodama Y., and Yamamoto F., 2007, “Skin Friction Reduction by Large Air Bubbles in a Horizontal Channel Flow”, Int. Journal of Multiphase Flow, Vol. 33, pp. 147-163.
- Murphy, J, Morgan, G. and Power, O., 2006, “Literature Review on the Impacts of Boat Wash on the Heritage or Ireland's Inland Waterways”, The Heritage Council of Ireland Series.



- Nakajima, Y., 1952, "On the Effect of Wind on the Manoeuvrability of Train Ferries," J. Society of Naval Architects of Japan, No.84, pp. 69-79.
- Nangia, R.K., Lumsden, R.B., 2004, "Novel Vortex Flow Devices - Columnar Vortex Generators Studies for Airwakes," AIAA-2004-2348.
- Neu, W.L., Good, N. and Klasén, E., 2007, "The Effect of Synthesis Model Uncertainties in Ship Design Optimization", 6th Int. Conf. on Computer Applications and Information Technology in the Maritime Industries (Compit'07), Cortona (Italy), 316-330.
- Nimura, T., Fujiwara, T., Ueno, M., Nonaka, K., 1997, "Wind Loads and Flow Visualization around an Oil Tanker Model," J. The Visualization Society of Japan, Vol. 17 (2), pp. 217-220.
- Noack, R., 2005, "SUGGAR: A General Capability for Moving Body Overset Grid Assembly," AIAA Paper 2005-5117, Proc. AIAA 17th CFD Conf., Toronto, Ontario, Canada.
- Noack, R., 2007, "Enabling Large Amplitude and Relative Motions Through Overlapping Grids," Proc. 9th Int. Conf. Numerical Ship Hydrodynamics, Ann Arbor, MI, USA.
- Noblesse F., Delhommeau D., Guilbaud M., Hendrix D., and Karafiath G., 2006, "Analytical and Experimental Study of Unsteady and Overturning Ship Bow Waves", Proc. 26th Symposium on Naval Hydrodynamics, Rome, Italy.
- Noblesse, F. & Yang C. 2006, 'Alternative Representations of Steady Potential Flow About a Ship', Proc. Of the 7th Int. Conf. on Hydrodynamics (ICHHD), Italy.
- Oberkampf, W.L., Trucano, T.G, Hirsch, C., 2004, "Verification, Validation and Predictive Capability in Computational Engineering and Physics," Applied Mechanics Reviews, Vol. 57, pp. 345-384.
- Oger, G, Doring, M., Alessandrini, B., Ferrant, P., 2006, "3D Wave Resistance Simulations Using Smoothed Particle Hydrodynamics," Proc. 26th Symp. Naval Hydrodynamics, Rome, Italy.
- Okada, S., 1957, "On the Heeling Moment due to the Wind Pressure on Small Vessels," J. Society of Naval Architects of Japan, No.92, pp. 75-81.
- Osaka, H., Kameda, T., Mochizuki, S., 1996, "Local Skin Friction Coefficient Evaluated Direct Measurement Method and Mean Flow Quantities in a Turbulent Boundary Layer," Trans. of JSME Series B, Vol. 62, No. 598, pp. 2230-2237.
- Paik B.G., Lee C.M., and Lee S.J., 2005, "Comparative Measurements on the Flow Structure of a Marine Propeller Wake Between an Open Free Surface and Closed Surface Flows", Journal of Marine Science and Technology, Vol. 10, pp. 123-130.
- Parnell, K.E., McDonald, S.C. and Burke, A., 2007, "Shoreline Effects of Vessel Wakes", Journal of Coastal Research, SI 50.
- Parsons, M.G. and Scott, R.L., 2004, "Formulation of Multicriterion Design Optimization Problems for Solution with Scalar Numerical Optimization Methods", J. Ship Res., 48(1), 61-76.
- Parsons, M.G., Singer, D.J. and Gaal C.M., 2006, "Multicriterion Optimization of Stern Flap Design", Marine Technology, Vol. 43 (1), 42-54.
- Pérez, F., Suárez, J., Clemente, J.A. and Souto, A., 2007, "Geometric Modeling of Bulbous Bow with the use on Non-Uniform Rational B-Spline Surfaces", J Mar. Sci. Technol., Vol 12, 83-94.

- Peri, D. and Campana, E.F., 2005, "High-fidelity Models and Multiobjective Global Optimization Algorithms in Simulation Based Design", J. Ship Res., 49(3), 159-175.
- Permanent International Association of Navigation Congresses (PIANC), 2003, "Guidelines for Managing Wake Wash from High-speed Vessels", Permanent International Association of Navigation Congresses (PIANC).
- Perret L., Braud P., Fourment C., David L., and Delville J., 2006, "3-Component Acceleration Field Measurement by Dual-Time Stereoscopic Particle Image Velocimetry", Experiments in Fluids, Vol. 40, pp. 813-824.
- Perrin R., Cid E., Cazin S., Sevrain A., Braza M., Moradei F., and Harran G., 2007, "Phase-Averaged Measurements of the Turbulence Properties in the Near Wake of a Circular Cylinder at High Reynolds Number by 2C-PIV and 3C-PIV", Experiments in Fluids, Vol. 42, pp. 93-109.
- Phillips, S. and Hook, D., 2006, "Wash from Ships as they Approach the Coast", RINA International Conference on Coastal Ships and Inland Waterways.
- Platt, J.R., 1998, "Wind Detection in a Microcosm: Ship/Aircraft Environment Sensors," Aerospace and Electronic Systems Magazine, IEEE Vol. 13, Issue 2, pp. 26-33.
- Poli, R., Kennedy, J. and Blackwell, T., 2007, "Particle Swarm Optimization: an Overview", Swarm Intell., 1, 33-57.
- Polsky, S.A., 2002, "A Computational Study of Unsteady Ship Airwake," AIAA-2002-1022.
- Popinet, S., Smithy, M., Stevensz, C., 2004, "Experimental and Numerical Study of the Turbulence Characteristics of Airflow around a Research Vessel," J. Atmospheric and Oceanic Tech., Vol. 21, pp. 1575-1589.
- Queutey, P. and Visonneau, M., 2007, "An Interface Capturing Method for Free-Surface Hydrodynamic Flows," Computers and Fluids, Vol. 36, pp. 1481 - 1510.
- Ragab, S.A., 2004, "Shape Optimization of Surface Ships in Potential Flow using an Adjoint Formulation", AIAA Journal, vol. 42 (2), 296-308.
- Rajagopalan, G., Schaller, D., Wadcock, A.J., 2005, "Experimental and Computational Simulation of a Model Ship in a Wind Tunnel," AIAA 2005-1347.
- Ramamurti, R., Sandberg, W.C., 2002, "Unstructured Grids for Ship Unsteady Airwakes: A Successful Validation," Naval Engineering Journal, Vol. 114 (4), pp. 41-53.
- Raven, H.C., van der Ploeg, A. and Eca, L., 2006, "Extending the Benefit of CFD Tools in Ship Design and Performance Prediction," ICHHD 7th International Conference on Hydrodynamics.
- Reddy, K.R., Tooletto, R., Jones, K.R.W., 2000, "Numerical Simulation of Ship Airwake," Computers & Fluids, Vol. 29, pp. 451-465.
- Regnstrom, B. and Bathfield, N., 2006, "Drag and Wake Prediction for Ships with Appendages Using an Overlapping Grid Method," Proc. 26th Symp. Naval Hydrodynamics, Rome, Italy.
- Rice J.R., Walker D., Fu T.C., Karion A., and Ratcliffe T., 2004, "Quantitative Characterization of the Free Surface around Surface Ships", Proc. 25th Symposium on Naval Hydrodynamics, St. John's, Newfoundland and Labrador, Canada
- Robbins, A. and Renilson, M.R., 2006, "A Tool for the Prediction of Wave Wake", RINA Transactions, Part A1, International Journal of Maritime Engineering



- Robbins, A., Thomas, G., Macfarlane, G.J., Renilson, M.R. and Dand, I., 2007, "The Decay of Catamaran Wave Wake in Deep and Shallow Water", International Conference on Fast Sea Transportation (FAST 2007).
- Roy, C.J., 2005, "Review of Code and Solution Verification Procedures for Computational Simulation," Journal of Computational Physics, Vol. 205, pp. 131-156.
- Ryu Y., Chang K.-A., and Lim H.J., 2005, "Use of Bubble Image Velocimetry for Measurement of Plunging Wave Impinging on Structure and Associated Greenwater" Measurement Science and Technology, Vol. 16, pp. 1945-1953.
- Sakamoto, N., Wilson, R.V. and Stern, F., 2007, "Reynolds-Averaged Navier-Stokes Simulations for High-Speed Wigley Hull in Deep and Shallow Water", Journal of Ship Research, Volume 51, No. 3, Sept.
- Salari, K. and Knupp, P., 2000, "Code Verification by the Method of Manufactured Solutions," Report SAND2000-1444, Sandia National Laboratories.
- Salas, M., 2006, "Some Observations on Grid Convergence," Computers & Fluids, Vol. 35, pp. 688-692.
- Samareh, J.A., 2005, "Geometry and Grid/Mesh Generation Issues for CFD and CSM Shape Optimization", Optimization & Engineering, Vol. 6, 21-32.
- Sanders W.C., Winkel E.S., Dowling D. R., Perlin M., and Ceccio S. L., 2006, "Bubble Friction Drag Reduction in a High-Reynolds Number Flat-Plate Turbulent Boundary Layer", Journal of Fluid Mechanics, Vol. 552, pp. 353-380.
- Sato, Y., Uzawa, K. and Miyata, H., 2007, "Validation of Motion Prediction Method for Trimaran Vessels," Proc. 9th Int. Conf. Numerical Ship Hydrodynamics, Ann Arbor, MI, United States.
- Schoenherr, K.E., 1932, "Resistance of Flat Surfaces," Trans. SNAME, Vol. 40, pp. 279-313.
- Sederberg, T.W. and Parry, S.R., 1986, "Free-Form Deformation of Solid Geometric Models", SIGGRAPH '86, Volume 20, pp. 269-278, ACM.
- Sezaki, Y., 1980, "Effects of the Wind Force to the Speed of a Car Carrier," J. Kansai Society of Naval Architects, Japan, No. 179, pp. 13-17.
- Sezer-Uzol, N., Sharma, A., Long, L.N., 2005, "Computational Fluid Dynamics Simulations of Ship Airwake," Proc. IMechE Vol. 219 Part G: J. Aerospace Engineering, pp. 369-392.
- Shafer, D.M, Ghee, T.A., 2005, "Active and Passive Flow Control over the Flight Deck of Small Naval Vessels," AIAA-2005-5265.
- Sharma, A., Long, L.N., 2001, "Airwake simulations on an LPD 17 ship," AIAA-2001-2589.
- Shearer, K.D.A., 1961, "Wind Tunnel Tests on Models of Merchant Ships," I.S.P. Vol.8, No.78, pp. 62-80.
- Shen X.C., Ceccio S.L., and Perlin M., 2006, "Influence of Bubble Size on Micro-Bubble Drag Reduction", Experiments in Fluids, Vol. 41, pp. 415-424.
- Shipman, J., Arunajatesan, S., Menchini, C., Sinha, N., 2005, "Ship Airwake Sensitivities To Modeling Parameters," AIAA-2005-1105.
- Shiraishi, N., Matsumoto, M., Shirato, H., Ishizaki, H., Osada, M., Matsui, T., 1986, "On Aerodynamic Stability Effects for

- Bluff Rectangular Cylinders by Their Corners Cut,” Proc. Symposium on Wind Engineering, Japan, pp. 193-198.
- Silva, M.J., Yamauchi, G.K., Wadcock, A.J., Long, K.R., 2004, “Wind Tunnel Investigation of the Aerodynamic Interactions Between Helicopters and Tiltrotors in a Shipboard Environment,” Presented at the American Helicopter Society 4th Decennial Specialist’s Conference on Aeromechanics, San Francisco, CA, January 21-23, 2004.
- Smith, D.W., Walker, J.H., 1959, “Skin Friction Measurements in Incompressible Flow,” NACA R-26.
- Soding, H., 2006, “Far Field Ship Waves”, Ship Technology Research, Vol 53, No. 3.
- Song Y.Y., Kim M.C., and Chun H.H., 2007, “A Study on Resistance Test of Icebreaker with Synthetic Ice”, Journal of the Society of Naval Architects of Korea, Vol.44, No.4, pp.389-397.
- Soomere, T., 2005, “Fast Ferry Traffic as a Qualitatively New Forcing Factor of Environmental Processes in Non-Tidal Sea Areas: A Case Study in Tallinn Bay, Baltic Sea”, Environmental Fluid Mechanics, Vol. 5.
- Soomere, T., 2006, “Nonlinear Ship Wake Waves as a Model of Rogue Waves and a Source of Danger to the Coastal Environment: A Review”, Oceanologia, Vol. 48.
- Soomere, T., 2007, “Nonlinear Components of Ship Wake Waves”, ASME Transactions, Volume 60, May.
- Soomere, T. and Engelbrecht, J., 2006, “Weakly Two-Dimensional Interaction of Solitons in Shallow Water”, European Journal of Mechanics B/Fluids, 25.
- Soomere, T., Poder, R., Rannat, K. and Kask, K., 2005, “Profiles of Waves from High-Speed Ferries in the Coastal Area”, Proc. Est. Acad. Sci. Eng., 11.
- Starke A.R., Windt J., and Raven H.C., 2006, “Validation of Viscous Flow and Wake Field Predictions for Ships at Full Scale”, Proc. 26th Symposium on Naval Hydrodynamics, Rome, Italy.
- Stern, F., Olivieri, A., Shao, J., Longo, J., and Ratcliffe, T., 2005 “Statistical Approach for Estimating Intervals of Certification or Biases of Facilities or Measurement Systems Including Uncertainties,” ASME J. Fluids Eng, Vol. 127, No. 2, May 2005, pp. 604-610
- Stern, F., Carrica P., Kandasamy M., Gorski J., O’Dea J., Hughes M., Miller R., Hendrix D., Kring D., Milewski W., Hoffman R. and Cary, C., 2006a, “Computational Hydrodynamic Tools for High-Speed Sealift”, SNAME Transactions, Vol. 114, pp. 55 – 81.
- Stern F., Huang J., Carrica P., Yang J., Ghosh S., and Van S., 2006b, “Two-Phase CFD and PIV EFD for Plunging Breaking Waves, Including Alternative CFD Approaches and Extensions for Air/Water Ship Flow”, Proc. 26th Symposium on Naval Hydrodynamics, Rome, Italy.
- Stern, F., Wilson, R., Shao, J., 2006c, “Quantitative V&V of CFD Simulations and Certification of CFD Codes,” International Journal for Numerical Methods in Fluids, Vol 50, pp. 1335-1355.
- Sur T.W. and Chevalier K., 2004, “Field Measurement of Bow Spray Droplets”, Proc. 25th Symposium on Naval Hydrodynamics, St. John’s, Newfoundland and Labrador, Canada.
- Syms, G.F., 2003, “Simulation of Ship Airwakes using a Lattice Boltzmann



- Method,” CFD2003, Vancouver, BC.
- Syms., G.F., 2004, “Numerical Simulation of Frigate Airwakes,” Int. J. Computational Fluid Dynamics, Vol. 18 (2), pp. 199-207.
- Tahara, Y., Wilson, R. V., Carrica, P. M., and Stern, F., 2006, “RANS Simulation of a Container Ship with Overset Grids and the Prognosis for Extension to a Self-P propulsion Simulator,” J. Marine Science & Tech., Vol. 11, pp. 209 – 228.
- Tahara, Y., Campana, E.F., Peri, D., Pinto, A., Kandasamy, M. and Stern, F., 2007, “Global Optimization and Variable Fidelity Strategies in the Single and Multiobjective Optimal Design of Fast Multihull Ships”, 9th Int. Conf. on Numerical Ship Hydrodynamics, Ann Arbor (USA).
- Takizawa, K., Tanizawa, K., Yabe, T., and Tezduyar, T. E., 2007, “Ship Hydrodynamics Computations with the CIP Method based on Adaptive Soroban Grids,” Int. J. Numer. Meth. Fluids, Vol. 54, pp. 1011 – 1019.
- Tanaka, A., Tamagami, Y., Yamashita, Y., Misumi, E., 1980, “The Ship Manoeuvrability in Strong Wind,” J. Kansai Society of Naval Architects, Japan, No. 176, pp. 1-10.
- Terrill E.J. and Taylor G.L., 2007, “Measuring Waves at Sea for the Validation of Wave Generation and Seakeeping Codes”, Proc. 9th International Conference on Numerical Ship Hydrodynamics, Ann Arbor, Michigan.
- Torsvik, T., 2006, “Long Wave Models with Application to High-Speed Vessels in Shallow Water”, Ph.D Thesis, University of Bergen, Norway.
- Torsvik, T., Dysthe, K. and Pedersen, 2006, “Influence of Variable Froude Number on Waves Generated by Ships in Shallow Water”, Physics of Fluids, Vol. 18.
- Toxopeus, S.L., 2005, “Verification and Validation of Calculations of the Viscous Flow around KVLCC2M in Oblique Motion,” 5th Osaka Colloquium, Osaka, Japan.
- Trosset, M.W., Alexandrov, N.M. and Watson, L.T., 2003, “New Methods for Robust Design Using Computer Simulations”, Proc. Section on Physical and Engineering Sciences, American Statistical Association.
- Troy C.D. and Koseff J.R., 2005, “The Generation and Quantitative Visualization of Breaking Internal Waves”, Experiments in Fluids, Vol. 38, pp. 549-562.
- Tsuji, T., Takaishi, Y., Kan, M., Sato, T., 1970, “Model Test about Wind Forces Acting on the Ships,” Ship Research Institute Report, Japan, Vol. 7, No.5, pp. 13-37 (209-233).
- Varyani, K.S., 2006, “Full Scale Study of the Wash of High Speed Craft”, Ocean Engineering, 33.
- Veelo, B.N., 2004, “Shape Modification of Ship Hulls in H-rep”, Ship Technology Research, Vol. 51, 162-172.
- Velegrakis, A.F., Vousdoukas, A.M, Vagenas, A.M, Karambas, T., Dimou, K. and Zarkadas, T., 2006, “Field Observations of Waves Generated by Passing Ships: A Note”, Coastal Engineering, Vol. 54.
- Visonneau, M., Deng, G. B., and Queutey, P., 2006, “Computation of Model and Full Scale Flows Around Fully-Appended Ships with an Unstructured RANSE Solver,” Proc. 26th Symp. Naval Hydrodynamics, Rome, Italy.
- Wakefield, N.H., Newman, S.J., Wilson, P.A., 2002, “Helicopter Flight around a ship’s superstructure,” Proc. Instn Mech Engrs, Vol. 216 Part G: J Aerospace Engineering, pp. 13-28.

- Wanger, B., 1967, "Windkraefte an Ueberwasserschiffen," JSTG 61. Band 1967, pp 226-250 (or Schiff und Hafen, pp. 894-900).
- Werner, S., 2006, "Computational Hydrodynamics Applied to an America's Cup Class Keel - Best Practice and Validation of Methods", Doctoral dissertation, Chalmers University of Technology, Gothenburg, Sweden.
- Wilson, R.V., Carrica, P.M. and Stern, F., 2006, "Unsteady RANS Method for Ship Motions with Application to Roll for a Surface Combatant," Computers & Fluids, Vol. 35, pp. 501-524.
- Wilson, R. V., Carrica P. M., and Stern, F., 2007a, "Simulations of Ship Breaking Bow Waves and Induced Vortices and Scars," Int. J. Numer. Meth. Fluids, Vol. 54, pp. 419 – 451.
- Wilson, R. V., Nichols, D. S., Mitchell, B., Karman, S. L., Betro, V. C., Hyams, D. G., Sreenivas, K., Taylor, L. K., Briley, W. R., and Whitfield, D. L., 2007b, "Simulation of a Surface Combatant with Dynamic Ship Maneuvers," Proc. 9th Int. Conf. Numerical Ship Hydrodynamics, Ann Arbor, MI, United States.
- Wilson, W., Fu, T. C., Fullerton, A. and Gorski, J., 2006, "The Measured and Predicted Wave Field of Model 5365: An Evaluation of Current CFD Capability," Proc. 26th Symp. Naval Hydrodynamics, Rome, Italy.
- Wood, M. P., Gonzalez, L. M., Izquierdo, J., Sarasquete, A. and Rojas, L. P., 2007, "RANSE with Free Surface Computations Around Fixed DTMB 5415 Model and Other Balino's Fishing Vessels," Proc. 9th Int. Conf. Numerical Ship Hydrodynamics, Ann Arbor, MI, United States.
- Wosnik M., Arndt R.E.A., and Ain Q., 2006, "Identification of Large Scale structures in the Wake of Cavitating Hydrofoils using LES and Time-resolved PIV", Proc. 26th Symposium on Naval Hydrodynamics, Rome, Italy.
- Xing, T., Kandasamy, M. and Stern, F., 2007, "Unsteady Free-Surface Wave-Induced Separation: Analysis of Turbulent Structures using Detached Eddy Simulation and Single-Phase Level Set," Journal of Turbulence, Vol. 8, No. 44.
- Yamano, T., Saito, Y., 1997, "An Estimation Method of Wind Forces Acting on Ships," J. Kansai Society of Naval Architects, Japan, No. 228, pp. 91-100.
- Yang, C., Kim, H. Y. and Noblesse, F., 2007, "A Practical Method for Evaluating Steady Flow About a Ship," 9th Int. Conf. on Fast Sea Transportation FAST2007, Shanghai, China.
- Yang, J., Sakamoto, N., Wang, Z., Carrica, P., and Stern, F., 2007, "Two-Phase Level-Set/Immersed-Boundary Cartesian Grid Method for Ship Hydrodynamics," Proc. 9th Int. Conf. Numerical Ship Hydrodynamics, Ann Arbor, MI, United States.
- Yoneta, K., Januma, S., Karasuno, K., 1992, "Analysis of Vessel's Wind Forces through the Utilization of a Physical-Mathematical Model - II," J. Society of Navigation of Japan, No. 86, pp. 169-177.
- Yoshimura, Y., Nagashima, J., 1985, "Estimation of the Manoeuvring Behaviour of Ship in Uniform Wind," J. Society of Naval Architects of Japan, No. 158, pp. 125-136.
- Zalek, S.F., Parsons M.G. and Beck R.F., 2006, "Evolutionary Multicriterion Optimization for Propulsion and Seakeeping", 26th ONR Symp. on Naval Hydrodynamics, Rome Italy.